Accepted Manuscript

On the nonexistence of degenerate phase-shift multibreathers in Klein-Gordon models with interactions beyond nearest neighbors

T. Penati, V. Koukouloyannis, M. Sansottera, P.G. Kevrekidis, S. Paleari

PII: S0167-2789(18)30113-1
DOI: https://doi.org/10.1016/j.physd.2019.06.002
Reference: PHYSD 32136

To appear in: *Physica D*

Received date : 6 March 2018
Revised date : 21 May 2019
Accepted date : 3 June 2019

Please cite this article as: T. Penati, V. Koukouloyannis, M. Sansottera et al., On the nonexistence of degenerate phase-shift multibreathers in Klein-Gordon models with interactions beyond nearest neighbors, *Physica D* (2019), https://doi.org/10.1016/j.physd.2019.06.002

On the nonexistence of degenerate phase-shift multibreathers in Klein-Gordon models with interactions beyond nearest neighbors

T. Penati[a,b], V. Koukouloyannis[c], M. Sansottera[a,b], P.G. Kevrekidis[d], S. Paleari[a,b]

[a] *Department of Mathematics "F.Enriques", Milano University, via Saldini 50, 20133 - Milano, Italy*
[b] *GNFM (Gruppo Nazionale di Fisica Matematica) – Indam (Istituto Nazionale di Alta Matematica "F. Severi"), Roma, Italy*
[c] *Department of Mathematics, Statistics and Physics, College of Arts and Sciences, Qatar University, P.O. Box 2713, Doha, Qatar*
[d] *Department of Mathematics and Statistics, University of Massachusetts, Amherst, MA 01003-4515, USA*

Abstract

In this work, we study the existence of, low amplitude, phase-shift multibreathers for small values of the linear coupling in Klein-Gordon chains with interactions beyond the classical nearest-neighbor (NN) ones. In the proper parameter regimes, the considered lattices bear connections to models beyond one spatial dimension, namely the so-called zigzag lattice, as well as the two-dimensional square lattice or coupled chains. We examine initially the necessary persistence conditions of the system derived by the so-called Effective Hamiltonian Method, in order to seek for unperturbed solutions whose continuation is feasible. Although this approach provides useful insights, in the presence of degeneracy, it does not allow us to determine if they constitute true solutions of our system. In order to overcome this obstacle, we follow a different route. By means of a Lyapunov-Schmidt decomposition, we are able to establish that the bifurcation equation for our models can be considered, in the small energy and small coupling regime, as a perturbation of a corresponding, beyond nearest-neighbor, discrete nonlinear Schrödinger equation. There, nonexistence results of degenerate phase-shift discrete solitons can be demonstrated by an additional Lyapunov-Schmidt decomposition, and translated to our original problem on the Klein-Gordon system. In this way, among other results, we can prove nonexistence of four-sites vortex-like waveforms in the zigzag Klein-Gordon model. Finally, briefly considering a one-dimensional model bearing similarities to the square lattice, we conclude that the above strategy is not sufficient for the proof of the existence or nonexistence of vortices due to the higher degeneracy of this configuration.

1. Introduction

The study of nonlinear dynamical lattices of Klein-Gordon (KG) and Fermi-Pasta-Ulam types has received considerable attention over the past two decades. This can be partially attributed to the intense interest in waveforms which are exponentially localized in space and periodic in time [8, 18]. Such discrete breather states have been recognized as emerging generically in systems that combine discreteness and nonlinearity. Relevant experimental examples abound and involve, e.g., Josephson junction arrays [6, 52], electrical transmission lines [16], micro-mechanical cantilever arrays [48, 49], coupled torsion pendula [12], coupled antiferromagnetic layers [50] and granular crystals [7, 10].

Most of these studies concern fundamental localized states. Typically also, they are predominantly in simpler, more controllable one-dimensional models [18]. However, optical [34], atomic [25], solid-state [14] and other settings suggest an interest in exploring higher-dimensional systems. Here, there may exist energy thresholds for breather existence [17]. Additionally, one can find novel discrete vortex structures [11, 13]. These are also referred to as phase-shift multibreathers. In fact, it may happen that higher charge vortices are more stable than their lower charge counterparts under appropriate conditions [27]. It has been argued that suitable adaptations of beyond-nearest-neighbor interactions [29] and the so-called zigzag [15] chains share some of the intriguing features of higher-dimensional settings. At the same time, such settings remain effectively one-dimensional in their formulation. For this reason, lattices with beyond-nearest-neighbor interactions represent a focal point in our study.

It is worthwhile to stress here that, on a more mathematical side, the proof of existence of these objects (discrete breathers and their variants that we consider in the present paper) is nowadays fairly standard in the limit of small coupling, provided a suitable nondegeneracy allows to apply the Implicit Function Theorem [35]. A key feature of our work is the development of a rather general technique to deal with degenerate situations, in order to prove existence or non-existence of continuation of solutions from the zero-coupling limit, when the standard approach does not work. Our technique will be shown to be applicable to several systems. Among them, the zigzag model is particularly relevant. This is because it represents a prototypical system for which a rather nontrivial form of degeneracy appears.

More specifically, in this work, we are interested in KG models with range of interactions beyond nearest-neighbor, with Hamiltonian

$$\mathscr{H} = \sum_{j\in\mathbb{Z}} \left[\left(\frac{1}{2} y_j^2 + V(x_j) \right) + \sum_{h=1}^{r} \epsilon_h \frac{(x_{j+h} - x_j)^2}{2} \right] .$$

In the present paper we will actually restrict to the case of the hard quartic potential, i.e.

$$V(s) = \frac{1}{2} s^2 + \frac{1}{4} s^4 , \tag{1}$$

although, in the limit of small enough amplitude, the results presented here hold true for generic symmetric potentials.

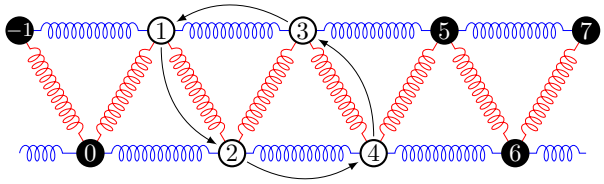

Figure 1: The two-dimensional zigzag model: all the interactions are nearest-neighbor ones with the same strength. The diagonal (red) springs are those which give the nearest-neighbor interaction in the corresponding one-dimensional version (see Figure 2), while the (blue) horizontal ones correspond to the next-to-nearest (NNN) neighbor interaction in that representation. The indexing indicates the energy flow of the vortex solutions. Color online.

The Hamiltonian above describes an infinite chain of anharmonic oscillators with linear interactions between them up to r neighbors and vanishing boundary conditions at infinity $\lim_{n\to\pm\infty} x_n = \lim_{n\to\pm\infty} y_n = 0$, which are automatically satisfied since we set $\ell^2(\mathbb{R}) \times \ell^2(\mathbb{R})$ as the phase space of the system. We will denote by E the energy of the system, i.e. the (conserved along the dynamics) value of the Hamiltonian $\mathscr{H}(x, y) = E$.

In what follows we will limit our analysis to range of interaction $r = 3$. By considering $\epsilon_j = k_j\epsilon$, with $k_1 = 1$, the above Hamiltonian becomes

$$\begin{aligned}\mathscr{H} =& \mathscr{H}_0 + \epsilon\mathscr{H}_1\\ \mathscr{H}_0 =& \sum_{j\in\mathbb{Z}} \left(\frac{y_j^2}{2} + V(x_j)\right)\\ \mathscr{H}_1 =& \frac{1}{2}\sum_{j\in\mathbb{Z}} \left[(x_j - x_{j+1})^2 + k_2(x_j - x_{j+2})^2 + k_3(x_j - x_{j+3})^2\right].\end{aligned} \tag{2}$$

We are interested in the existence, in the small coupling limit (i.e., for values of the coupling close to the anti-continuum limit [35] of $\epsilon \to 0$), of multibreather solutions. These constitute a class of periodic orbits whose energy is spatially localized on few oscillators (or sites). More precisely, we will denote by $S = \{j_1, j_2, \ldots, j_m\}$ the set of their indices. In the case of the zigzag model, four adjacent oscillators will be considered (namely with indices $j \in S = \{1, 2, 3, 4\}$; see Figures 1 and 2). If these four oscillators are given the same energy for $\epsilon = 0$, any orbit is periodic. This is so regardless of the phase differences between them. In this way, a completely resonant four-dimensional torus is formed for the zigzag system.

Our investigation can thus be seen to fall within the general question of the perturbation of low-dimensional invariant resonant tori in Hamiltonian dynamics: generically, only a finite number of periodic orbits are expected to survive to the breaking of the resonant torus. Lower bounds for the minimal number of such persisting solutions can be derived by means of geometric methods, such as in the so-called Moser-Weinstein theory (see [54, 38], but also Chapter 1 of [5] for a simpler exposition of main results in this direction). In the case of resonant tori of maximal dimension, classical results of perturbation theory due to Poincaré [46, 47] allow to identify these orbits as critical points of the averaged perturbation on a torus, under some suitable nondegeneracy conditions; degenerate cases, still considering tori of maximal dimension, have been instead the object of more recent papers, such as in [37, 53] or in [44], where normal form techniques and fixed point arguments were combined. One of the first extensions to low-dimensional tori can be found in [51], still under suitable nondegeneracy assumptions (see also [55] for a contemporary extension to multiscale systems). However, to our knowledge, none of the above results provides a constructive and applicable perturbation strategy. Thus, the object of the present investigation will be the proposal of such a strategy for the continuation of periodic orbits in the degenerate and low-dimensional case.

When we consider only nearest neighbors interactions in (2), i.e., setting $k_2 = k_3 = 0$, and consecutive oscillators, it is well known that only multibreathers with *standard phase-differences* ($\varphi = 0$ or π) between adjacent oscillators survive the breaking of the resonant torus [30]. If next-to-nearest (or longer range) neighbor interactions are added, other solutions with non-standard phase differences may survive: these are called *phase-shift* multibreathers (see e.g. [32, 43]). The emergence of phase-shift multibreathers in both one-dimensional KG and discrete nonlinear Schrödinger (dNLS) models with interactions beyond those of the nearest-neighbor interactions, have been investigated in some recent works [9, 24, 29]. This issue partially overlaps with the study of vortex structures in two-dimensional lattices, like in [13, 28, 41]. Indeed, a suitable beyond nearest neighbor interaction in a one-dimensional lattice allows to reproduce the local interactions involved in a two-dimensional vortex, for example in a hexagonal or square lattice, thus providing an emulation of the two-dimensional object by a one-dimensional one at leading order in the coupling perturbation parameter ϵ; such an approximation clearly fails at higher orders, due to the differences in terms of lattice shape and interaction among sites.

As an intermediate case between a one- and a two-dimensional lattice we can consider the aforementioned zigzag lattice [15]. This lattice can be seen to consist of just two oscillator chains which are connected as shown in Figure 1. In this case, we can easily see that *vortex* solutions of Figure 1 correspond to *four-site multibreathers* in the *one-dimensional* system of Figure 2. The zigzag system is described by a Hamiltonian

$$\begin{aligned}\mathscr{H}_{110} = \sum_{j\in\mathbb{Z}} \Bigg[&\left(\frac{1}{2}y_j^2 + \frac{1}{2}x_j^2 + \frac{1}{4}x_j^4\right) +\\ &+\frac{\epsilon}{2}\left((x_{j+1} - x_j)^2 + (x_{j+2} - x_j)^2\right)\Bigg],\end{aligned} \tag{3}$$

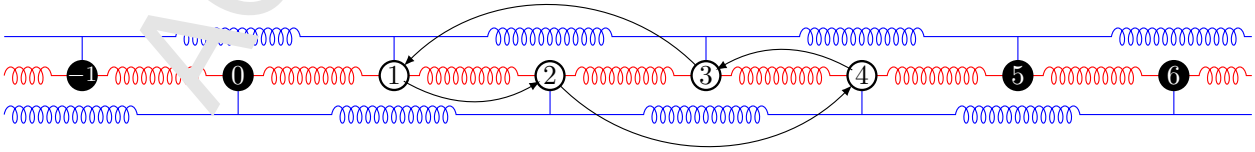

Figure 2: The corresponding one-dimensional zigzag model. The numbers indicate the correspondence to the two-dimensional zigzag model. For the color meaning, please refer to the caption of Figure 1. Color online.

that corresponds to a Hamiltonian (2) with $k_2 = 1$ and $k_3 = 0$. Indeed, the subscript of $\mathscr{H}$ refers to the values of the coupling constants k (including k_1 which is always 1 in our notation).

As we anticipated before, both in the one-dimensional and in the two-dimensional case, the existence of multibreathers is typically established via implicit function theorem arguments, which rely on the non-degeneracy of some linearized equation. This is the case, for example, of the classical result in [1], where true multibreather solutions are obtained from approximate solutions which correspond to critical points of an averaged (effective) Hamiltonian: in this context, an approximate solution has to satisfy some *persistence conditions* (see e.g. [29]) which select admissible candidates of phase-differences for a possible continuation. The same analytical tool, i.e., the implicit function theorem, can be used also in a different scheme: approaching the original problem with a Lyapunov-Schmidt decomposition (with the torus being resonant), it is used to solve the Range equation, and then the use of some symmetry, like time-reversibility, can remove the Kernel directions (see [43]). However, in some degenerate cases, the candidate solutions we get from the persistence conditions do not correspond to true solutions of our systems. In such cases, a deeper analysis is required which typically involves higher order terms of the bifurcation (kernel) equation.

In particular, by studying persistence conditions, one realizes that candidate solutions are not isolated in degenerate systems, but appear in families. In the following section it will be illustrated how a simple form of degeneracy arises when in the multibreather configuration there are holes between oscillators which are large in comparison with the interaction range. More subtle mechanisms are related to particular symmetries in the interactions beyond nearest neighbor ones even for consecutive sites configurations. A prototypical case is that of the zigzag system (3), for which we realize that the candidate vortex solutions of Figure 1 appear as two one-parameter families intersecting in two highly symmetric configurations.

To get a complete description of the continuation we exploit the corresponding dNLS model

$$H = \sum_{j\in\mathbb{Z}} \left[\left(|\psi_j|^2 + \frac{3}{8}|\psi_j|^4 \right) + \right. \tag{4}$$
$$\left. + \frac{\epsilon}{2}\left(|\psi_{j+1} - \psi_j|^2 + k_2|\psi_{j+2} - \psi_j|^2 + k_3|\psi_{j+3} - \psi_j|^2 \right) \right],$$

as a bridge to the KG system $\mathscr{H}$. Indeed, in the framework of resonant normal form theory, the former can be shown to be a good approximation of the latter in the energy regime $E \ll 1$ and for couplings $\epsilon \ll \sqrt{E}$ (see, e.g., [2, 42], or the proofs in Section 3); this means that by a close to the identity symplectic change of coordinates, the difference between the two models (2) and (4) is shown to be small as $\mathcal{O}(E^6 + \epsilon^2 E + |\epsilon| E^4)$ in some norm of analytic functions. Moreover, although the system H shares the same degeneracy as the original KG model $\mathscr{H}$, it is easier to derive the nonexistence of any phase-shift discrete soliton of H following the scheme of [45], by expanding its bifurcation equation to leading order and verifying a sufficient condition on it. Since such a condition is robust under small perturbations, we are then able to transfer the nonexistence result of H to the original system $\mathscr{H}$, showing the *nonexistence* of any vortex solution (symmetric or asymmetric) for the corresponding degenerate KG models, in the prescribed regime of the two main parameters E and ϵ.

We present here, among the possible statements, the one concerning the four-sites multibreathers for the zigzag model. We thus introduce the four-dimensional resonant torus filled by periodic orbits, belonging to the possible solutions of $\mathscr{H}_{110}$ for $\epsilon = 0$

$$\bar{u}_j(\tau) = \begin{cases} 0 \,, & j \notin S \\ x(\tau + \theta_j) \,, & j \in S \end{cases} , \tag{5}$$

with $S = \{1, 2, 3, 4\}$ and $x(\cdot)$ is a nonlinear oscillation of normalized period 2π

$$\gamma^2 x'' + x + x^3 = 0 \,, \qquad x(0) = \rho \,, \tag{6}$$

where $\tau := \gamma t$ is the rescaled time induced by the frequency γ associated to the (small) amplitude ρ of the oscillation; we also introduce the phase differences φ_j, between the above mentioned successive oscillators, as

$$\varphi_j := \theta_{j+1} - \theta_j \,, \quad j \in S^* = \{1, 2, 3\}. \tag{7}$$

As was previously mentioned, in this case, the configurations suitable for continuation lie in two one-parameter families within the three-dimensional manifold of phase-differences variables (7). These two families intersect in what we call *symmetric vortex* configuration, since it features the standard vortex phase differences $\Phi^{(\mathrm{sv})} \equiv \boldsymbol{\varphi} = \pm(\pi/2, \pi, -\pi/2)$, where $\boldsymbol{\varphi} = (\varphi_1, \varphi_2, \varphi_3)$, according to (7). The reason that the $\Phi^{(\mathrm{sv})}$ configuration is the one with $\pm(\pi/2, \pi, -\pi/2)$ and not the $\pm(\pi/2, \pi/2, \pi/2)$ as one could have expected, is that, as we can see from Figure 1, the vortex-flow is $1 \to 2 \to 4 \to 3 \to 1$ while the phase differences are calculated using consecutive oscillators. On the other hand, we will call all the other solutions of these two families, with $\boldsymbol{\varphi} \neq \Phi^{(\mathrm{sv})}$ as *asymmetric vortices*. Let us note here that these families also include some of the standard ($\varphi_i \in \{0, \pi\}$) multibreather solutions in addition to the isolated standard solutions of the persistence conditions. The next theorem claims that these standard multibreathers are the only periodic orbits persisting under a small perturbation effect, and thus no phase-shift multibreathers exist upon continuation from the zero-coupling limit, in the small amplitude regime.

Theorem 1.1. *For ϵ and ρ small enough ($\epsilon \neq 0$), the only four-site unperturbed solutions* (5) *that can be continued, at fixed frequency γ, to solutions $u_j(\rho, \epsilon, \tau)$ of* (3)*, correspond to $\varphi_j \in \{0, \pi\}$.*

Moreover, in all the cases which appear to be non-degenerate, the "dNLS approximation" strategy, allows to derive any existence result for (2) from the existence result for the corresponding dNLS model (4). The implementation of this transfer-of-results technology between the dNLS and the corresponding KG lattices is one of the central contributions of the present work. The price one has to pay for the use of this strategy lies in the restrictions in the regime of parameters for which the models (2) are well approximated by the corresponding averaged normal forms (4).

It is important to remark that degeneracy may appear with different "degrees" (see Definition 3.2). Indeed, within the family (2), a very degenerate system is given by the Hamiltonian $\mathscr{H}_{101}$ (see (17)) which has $k_2 = 0$ and $k_3 = 1$ and it is used to offer insights towards vortex-like configurations in

two-dimensional square lattices (due to the absence of diagonal interactions when considering 4 nodes as lying at the vertices of a square). This system admits, at the level of the persistence condition, three vortex families, having the symmetric vortex configuration in their triple intersection, giving thus a high degree of degeneracy. We stress that the corresponding dNLS model is exactly the one studied in [45], but within the scheme implemented in the present paper, the high degree of degeneracy of $\mathscr{H}_{101}$ does not allow us to transfer the nonexistence result proved in [45] to the corresponding KG chain. We are presently exploring a different normal form strategy which works directly on the original KG model and interprets the problem in the classical sense of breaking of a completely resonant low-dimensional torus [44].

Due to the degeneracy, which manifests itself through the presence of families of candidate solutions, and even more through their intersection points, we attempt to complement our analysis by performing a numerical investigation of the persistence conditions of the full problem (2) in the neighborhood of the parameter-values $(k_2, k_3) = (1, 0)$ and $(k_2, k_3) = (0, 1)$, which correspond to the zigzag and $\mathscr{H}_{101}$ configurations. In this study, we realize there exist families of solutions in the (k_2, k_3)-space which are non-degenerate and consequently easily continued to real solutions. But, as the k-parameters converge to the above mentioned set of values, the originally non-degenerate families become degenerate and the persistence conditions cannot provide a definite answer on the existence or not of the corresponding multibreather configurations.

This paper is structured as follows. In Section 2 we discuss the problem of degeneracy, reviewing the classical Effective Hamiltonian Method, and providing several examples of degenerate and non-degenerate systems. The core of the mathematical content of the paper is in Section 3, where after some settings and a precise definition of degeneracy (see Definition 3.2), the abstract results (Theorems 3.1 and 3.2) are formulated. The proofs, described by an extensive roadmap, and divided in three main steps, follow in a subsequent subsection. In Section 4, by applying the previous general statements, existence and nonexistence results are proved for the various models presented in Section 2. The numerical explorations of the persistence conditions close to the parametric regions which correspond to the zigzag and $\mathscr{H}_{101}$ systems are reported in Section 5. Finally, Section 6 includes some concluding remarks about possible future directions on the topic.

2. The problem of degeneracy

In the present Section we discuss the main mathematical issue, i.e. the presence of degeneracy, which motivates the developments discussed in the present paper. In particular, we will define what we mean by degeneracy presenting a classical technique used to discuss the existence of multibreathers (MB): among the requested hypothesis for the result to hold, we will emphasize the "non degeneracy" one.

Then, after presenting a simple non-degenerate case, we will show two different types of configurations which lead to degeneracies.

2.1. The Effective Hamiltonian Method

Here we review the Effective Hamiltonian Method for the investigation of the existence of multibreather solutions introduced in [3], extended in [1, 36], and revisited and applied in several papers, like e.g. [29, 31, 32, 33].

We very briefly recall that the idea behind such a method is to calculate the critical points of an "effective" Hamiltonian $\mathscr{H}_{\text{eff}}$ which are in a one-to-one correspondence with the multibreather periodic orbits of the original system.

First, we consider the m oscillators (sometimes referred to as "central", a term we avoid here since it may generate confusion in the case of non-consecutive configurations) which are involved in the MB and enumerate them according to the set $S = \{j_1, j_2, \dots, j_m\}$. Here we are adopting a general enumeration of the "active" oscillators in order to be able to consider not only adjacent oscillators, but also configurations with "holes" between them in what follows. In the uncoupled limit $\epsilon = 0$ we consider them moving in periodic orbits with the same frequency but arbitrary initial phase. Then, in order to better detail the procedure, we introduce action-angle variables (J, θ), through the displacement equation of an individual central oscillator:

$$x(\theta, J) = \sum_{n=1}^{\infty} A_{n-1}(J) \cos[(2n-1)\theta] \ . \tag{8}$$

The lack of the even terms A_{2n} in the Fourier expansion stems from the symmetry of the potential V. We thus get a Hamiltonian $\mathscr{H}(x_i, y_i, J_j, \theta_j, \epsilon)$, with $j \in S$ and $i \in \mathbb{Z} \setminus S$. Now, with an additional linear canonical transformation we introduce a new set of action-angle variables

$$\begin{aligned} &\vartheta = \theta_{j_1} \ , && A = \sum_{k=1}^{m} J_{j_k} \ , \\ &\varphi_\ell = \theta_{j_{\ell+1}} - \theta_{j_\ell} \ , && I_\ell = \sum_{k=\ell+1}^{m} J_{j_k} \ , \qquad \ell = 1, \dots, m-1 \ , \end{aligned} \tag{9}$$

with φ_ℓ representing the phase differences between "consecutive" (within S, according to our enumeration) sites. The above set of coordinates represents the natural introduction of $m-1$ slow angles φ_l and a fast angle ϑ, associated to the resonances among the equally excited oscillators: indeed, since at $\epsilon = 0$ we consider the oscillators J_l, $l \in S$ with the same action J^* (in order to have also the same frequency), they lie in the so-called $1:1$ resonance.

With the Hamiltonian in the form $\mathscr{H}(\vartheta, A, \varphi_\ell, I_\ell, x_i, y_i, \epsilon)$, it is possible to introduce the effective Hamiltonian as

$$\mathscr{H}_{\text{eff}} := \frac{1}{T} \oint \mathscr{H} \circ z(t) dt \ ,$$

where z is a periodic trajectory in the phase space obtained, as illustrated in [1], by a continuation procedure, at constant A, starting from the object defined in the $\epsilon = 0$ limit.

From a practical point of view, $\mathscr{H}_{\text{eff}}$ being defined in terms of an object (the closed path z) which is not known explicitly, the relation between MB solutions and the critical points of $\mathscr{H}_{\text{eff}}$ seems useless. Here comes the role of (non)degeneracy. Indeed, expanding everything in powers of ϵ, at the leading order the effective Hamiltonian can be calculated explicitly using z_0, the periodic orbit in the uncoupled limit. If the critical points found in such a case are non-degenerate, they can be continued to critical points of the full effective Hamiltonian, i.e. to true MB solutions.

Since by construction $\mathscr{H}_{\text{eff}}$ does not depend on ϑ, then A is constant and will be omitted. Recalling the general structure of

(2) the leading order of the effective Hamiltonian is simply the sum of the uncoupled Hamiltonian $\mathscr{H}_0$ (which depends solely on the actions being the integrable part of the Hamiltonian) plus the average $\langle\mathscr{H}_1\rangle$ of the coupling terms with respect to the uncoupled periodic orbits:

$$\mathscr{H}_{\rm eff}(\varphi_\ell, I_\ell, \epsilon) = \mathscr{H}_0(I_\ell) + \epsilon\langle\mathscr{H}_1\rangle(\varphi_\ell, I_\ell) + \mathcal{O}(\epsilon^2) \ ,$$

where

$$\langle\mathscr{H}_1\rangle(\varphi_\ell, I_\ell) := \frac{1}{T}\oint \mathscr{H}\circ z_0(t)dt \ .$$

Critical points of the effective Hamiltonian can now be found as continuations, to nonzero ϵ, of non-degenerate equilibria (φ_l^*, I_l^*) of its leading order, with respect to ϵ, part. The values of the actions I_l^* correspond to the unperturbed solution $J_l = J^*$, while the existence of $\{\varphi_l^*\}$ is given by the *persistence (necessary) condition*

$$\mathcal{P}(\varphi) := \frac{\partial\langle\mathscr{H}_1\rangle}{\partial\varphi_l}\Big|_{I_l=I_l^*} = 0 \ ; \tag{10}$$

the above condition provides critical points of $\langle\mathscr{H}_1\rangle(\varphi_l, I_l^*)$ on the torus $\mathbb{T}^{m-1}$ of the slow angles. Solutions φ^* of (10) such that $\varphi_l \in \{0, \pi\}$ will be referred to as *standard* configurations, while in the $\varphi_l \notin \{0, \pi\}$ case they will be called *phase-shift* configurations. The possibility of their continuation is given by the following set of *non degeneracy conditions* at (φ_l^*, I_l^*)

$$\left|\frac{\partial^2\mathscr{H}_0}{\partial I_j\partial I_i}\right| \neq 0 \ , \tag{ND-K}$$

$$\left|\frac{\partial^2\langle\mathscr{H}_1\rangle}{\partial\varphi_j\partial\varphi_i}\right| \neq 0 \ , \tag{ND-P}$$

$$\Omega \neq k\gamma \ , \tag{NR}$$

where $\Omega = V''(0)$ is the frequency of the small oscillations at the elliptic equilibrium of the anharmonic oscillator, and γ is the frequency of the periodic orbit we are looking for, and coincides with all the $\frac{\partial\mathscr{H}_0}{\partial J_j}\Big|_{J^*}$, which are all equal since we are in the 1:1 resonance. Instead of using numbers to refer to the above conditions, we use letters which remind to the name of the condition itself. Indeed condition (ND-K) is often known in the KAM literature as *Kolmogorov's nondegeneracy* (see for example the classical works [25, 26], and encodes the fact that the resonant torus is isolated in the space of actions; condition (ND-P) is instead known as *Poincaré nondegeneracy*, since it appears already in well-known results of continuations of periodic orbits due to Poincaré [45, 47]; and condition (NR) is a classical (*first Melnikov*) condition of nonresonance, needed to "remove" leading order interactions between action-angle variables (φ_l, I_l) and the transversal variables (x, y). With the above conditions, MB solutions can be obtained via Implicit Function Theorem.

Remark 2.1. *We stress now that in the class of models we are dealing with, both conditions* (ND-K) *and* (NR) *are obviously satisfied given the nonlinearity of the oscillators and their small amplitude (since for higher amplitudes we could have resonances and (NR) wouldn't hold). Thus, the actual nondegeneracy condition reduces to* (ND-P)*. Moreover, standard Multibreathers, corresponding to solutions φ^* of* (10) *with $\varphi_l^* \in \{0, \pi\}$, can be continued independently of the validity* (ND-P)*, as proved in [43].*

It is possible to exploit the introduction of action-angle variables (8) to give a more explicit expression of $\langle\mathscr{H}_1\rangle$ and its derivatives (see, e.g., [32] for a detailed derivation in the nearest-neighbor case): we will show it in the particular situations analyzed below.

In the following subsections we will first illustrate some typical examples of non-degenerate situations, and then we will investigate in some interesting cases the appearance of degeneracy through the two different mechanisms already mentioned in the Introduction.

2.2. Non-degenerate situations

Let us first show the actual implementation of the Effective Hamiltonian Method in some non-degenerate cases.

In particular let us recall that in the nearest-neighbor setting, with consecutive sites $S = \{1, \dots, m\}$, it is shown in [30, 32] that continuation from the zero coupling limit is possible only for standard configurations, i.e. the so called in/out of phase MB (see Figure 3 for an illustration of the possible configurations in the 3 sites case). In this case an explicit calculation brings the averaged Hamiltonian in the form

$$\langle\mathscr{H}_1\rangle = -\frac{1}{2}\sum_{j=1}^{m-1}\sum_{n=1}^{\infty} A_{2n-1}^2\cos[(2n-1)\varphi_j] \ ;$$

it is thus clear that $\varphi = 0, \pi$ are critical points for $\langle\mathscr{H}_1\rangle$; we refer again to the above quoted papers for the proof that these are the only configuration that can be continued.

Another example is the triangular configuration of consecutive sites $S = \{1, 2, 3\}$ in the zigzag model, i.e. with first and second neighbor interactions. For this configuration, one could also refer to the study of proper vortex solutions in two-dimensional lattices, e.g. [28, 33], since the corresponding effective Hamiltonian functions are equivalent at leading order of approximation. In this case we have

$$\langle\mathscr{H}_1\rangle = -\frac{1}{2}\sum_{n=1}^{\infty} A_{2n-1}^2\Big[\cos[(2n-1)\varphi_1] + \cos[(2n-1)\varphi_2] + \cos[(2n-1)(\varphi_1+\varphi_2)]\Big] \ ;$$

the persistence condition (10) is easily derived (see also Section 3 of [28]) and nondegeneracy (ND-P) is easily checked, showing

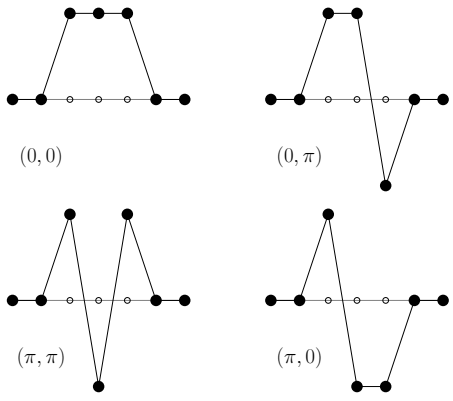

Figure 3: An example of the four possible 3-sites MB, in the uncoupled case, with different choices of the phase shifts (φ_1, φ_2).

that there exists an isolated phase shift MB with $\varphi = 2\pi/3$, i.e. a vortex solution.

As a last simple example of non degeneracy we might consider again the zigzag model as above, but in a configuration of non consecutive sites: $S = \{1, 3\}$ (see Table 1, bottom-left panel). We stress that in this case we have a hole from the point of view of the configuration, but due to the second neighbor interaction (see the blue spring among sites 1 and 3, in figure 1) actually there is no degeneracy at first order. Indeed, recalling our notation with enumerated sites $S = \{j_1, j_2\}$,

$$\langle \mathscr{H}_1 \rangle = -\frac{1}{2} \sum_{n=1}^{\infty} A_{2n-1}^2 \cos[(2n-1)\varphi_1] \ ,$$

with $\varphi_1 = \theta_3 - \theta_1$ the only phase difference available.

2.3. Degeneracy from "holes"

In this part we will show that suitable combination of configuration holes and interaction types may lead to "effective holes" at first order; this will generate in an obvious way a problem of degeneracy.

The first simple example is given by a chain with only nearest-neighbor interaction, and a configuration with a hole like $S = \{1, 3\}$ (see Table 1, top-right panel). Let us recall that in such a case the interaction part $\mathscr{H}_1$ contains only terms of the form $x_j x_{j+1}$, besides the quadratic terms x_j^2 which depend only on the actions. Thus performing the average along z_0 we have that $\oint x_0 x_1 = \oint x_1 x_2 = \oint x_2 x_3 = \oint x_3 x_4 = 0$ are all zero because in each product one of the factors is identically zero, since only x_1 and x_3 belong to the chosen configuration. The only contributing terms are the averages of x_1^2 and x_3^2:

$$\langle \mathscr{H}_1 \rangle = \frac{1}{T} \oint (x_1^2 + x_3^2) \circ z_0(t) dt = C(J^*) \ ,$$

where J^* are the fixed vales of the original actions of the unperturbed orbit z_0. Thus there is no dependence on the phase shifts φ, and this brings a complete degeneracy. Therefore it is not possible to proceed with the standard technique to check whether some configuration (and in the case, which ones) can be continued to the interacting regime $\epsilon \neq 0$.

Type of interaction	Presence of an "effective hole"	
	no	yes
NN		
NN+NNN	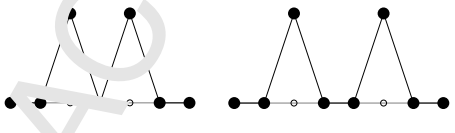	

Table 1: Possible configurations of a 2-sites MB, in the uncoupled case, with or without "holes". Supposing a NN interaction in the first row, and a NN+NNN interaction in the second one, the situations with "effective holes" are only in the second column.

A further example that, like the previous one, we will be able to deal with, using the results presented in the present paper, is given by a zigzag model (i.e. with first and second neighbor interaction having the same strength) and a double hole configuration $S = \{1, 4\}$ (see Table 1, bottom-right panel). Here the interaction part of the Hamiltonian contains terms (among those depending on the phases) of the form $x_j x_{j+1}$ and $x_j x_{j+2}$, but again we will have $\oint x_0 x_1 = \oint x_1 x_2 = \oint x_3 x_4 = \oint x_4 x_5 = 0$ and $\oint x_{-1} x_1 = \oint x_1 x_3 = \oint x_2 x_4 = \oint x_4 x_6 = 0$ for the same reason as before.

2.4. Hidden degeneracy in beyond-nearest-neighbor models: four-site vortex-like configurations

In the previous subsection we illustrated the appearance of a degeneracy whose source is very clear and somewhat elementary: the presence of an "effective hole", in the sense of both configuration and interaction, leads to the lack of some terms in the averaged Hamiltonian, thus trivially producing a degeneracy.

We here want to show a more subtle form of degeneracy which is not due to "holes", but is related to "internal symmetries" generated by beyond nearest-neighbor interactions and their relative strength. We will consider two examples, both with a 4 consecutive sites configuration $S = \{1, 2, 3, 4\}$: the first one will be again the zigzag model, while the second will be a model with first (NN) and third (next-to-next-nearest NNNN) neighbor interactions system.

We recall that both the above mentioned models belong to the family (2): the zigzag one is indeed given by $\mathscr{H}_{110}$ as in (3), and the second model will be accordingly denoted as $\mathscr{H}_{101}$ (see (17) later). Since we want to study structures with four central oscillators, only three phase differences φ_i between them are defined as in (7). The average value of the coupling term of the Hamiltonian (2) $\langle \mathscr{H}_1 \rangle$ is calculated along the unperturbed orbit and reads

$$\begin{aligned} \langle \mathscr{H}_1 \rangle = -\frac{1}{2} \sum_{m=1}^{\infty} A_m^2 \Big(& \cos(m\varphi_1) + \cos(m\varphi_2) + \cos(m\varphi_3) + \\ & + k_2 \big(\cos(m(\varphi_1 + \varphi_2)) + \cos(m(\varphi_2 + \varphi_3)) \big) \\ & + k_3 \cos(m(\varphi_1 + \varphi_2 + \varphi_3)) \Big) \ . \end{aligned}$$

2.4.1. The $\mathcal{H}_{110}$ (zigzag) model.

The persistence conditions (10) for the case of the zigzag system (3), i.e., with $k_2 = 1$ and $k_3 = 0$, read

$$\mathcal{P}_{110}(\varphi) \equiv \begin{cases} M(\varphi_1) + M(\varphi_1 + \varphi_2) = 0 \\ M(\varphi_2) + M(\varphi_1 + \varphi_2) + M(\varphi_3 + \varphi_2) = 0 \\ M(\varphi_3) + M(\varphi_2 + \varphi_3) = 0 \end{cases} \tag{11}$$

with

$$M(\varphi) \equiv \sum_{m=1}^{\infty} (2m-1) A_{2m-1}^2 \sin((2m-1)\varphi) \ , \tag{12}$$

with A_i as in (8).

Taking under consideration the symmetries of $M(\varphi)$

$$\begin{aligned} & M(\pi + \varphi) = -M(\varphi) \, , \qquad M(-\varphi) = -M(\varphi) = M(2\pi - \varphi) \, , \\ & M(\pi - \varphi) = +M(\varphi) \, , \qquad M(0) = M(\pi) = 0 \ , \end{aligned} \tag{13}$$

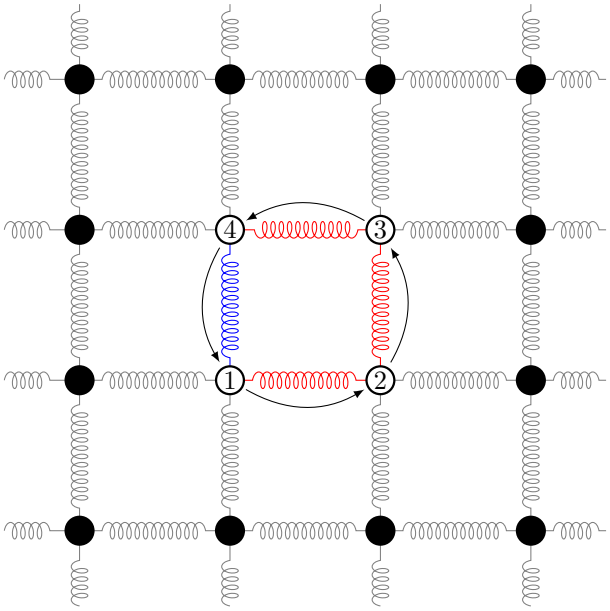

Figure 4: The two-dimensional square model and the 4-site MB. All the interactions are nearest neighbor ones with the same strength; in color the interactions involving only the MB, in particular in red those which correspond to nearest-neighbor in the one dimensional version (see Figure 5), in blue the one corresponding to the third neighbor; in grey the other interactions. The indexing indicates the energy flow of the vortex solutions. Color online.

it is straightforward to check that the persistence conditions for the zigzag-KG case, i.e., (11) and (12), admit two families of solutions

$$F_1 : \boldsymbol{\varphi} = (\varphi, \pi, -\varphi) \ , \qquad F_2 : \boldsymbol{\varphi} = (\varphi, \pi, \pi + \varphi) \ , \tag{14}$$

the members of which we call as *asymmetric vortices*. In addition, there exist also four standard isolated solutions $F_{\rm iso} = \boldsymbol{\varphi} \in \{(0,0,0), (0,0,\pi), (\pi,0,0), (\pi,0,\pi)\}$. The latter four solutions, being isolated, do not present difficulties concerning the application of standard techniques for their continuation. The former solutions, given by (14), present a clear degeneracy, i.e. (ND-P) is not satisfied, since they belong to a family and thus are not isolated.

In principle, all combinations of 0's and π's work trivially, since all the terms in the persistence condition simply vanish. We have to note here that the rest of the standard multibreather solutions are part of the F_1 and F_2 families.

It is important to stress that conditions (11) are necessary but not sufficient for the existence of multibreather solutions. Indeed, in order to continue to real solutions of (3), the corresponding Jacobian matrix $D_\varphi(\mathcal{P}_{110})$ needs to be non-degenerate, which is actually the (ND-P) condition. The matrix $D_\varphi(\mathcal{P}_{110})$ is given by

$$\begin{pmatrix} M'(\varphi_1)+M'(\varphi_1+\varphi_2) & M'(\varphi_1+\varphi_2) & 0 \\ M'(\varphi_1+\varphi_2) & M'(\varphi_2)+M'(\varphi_1+\varphi_2)+M'(\varphi_2+\varphi_3) & M'(\varphi_2+\varphi_3) \\ 0 & M'(\varphi_2+\varphi_3) & M'(\varphi_3)+M'(\varphi_2+\varphi_3) \end{pmatrix} ,$$

where $M'(\varphi) \equiv \sum_{m=1}^{\infty} (2m-1)^2 A_{2m-1}^2 \cos((2m-1)\varphi)$. By using the symmetries of $M'(\varphi)$

$$\begin{aligned} &M'(2\pi - \varphi) = M'(\varphi) = M'(-\varphi) \ , \\ &M'(\pi - \varphi) = M'(\pi + \varphi) = -M'(\varphi) \ , \\ &M'\left(\frac{3\pi}{2}\right) = M'\left(\frac{\pi}{2}\right) = 0 \ , \end{aligned} \tag{15}$$

it is easy to check that for the isolated solutions $F_{\rm iso}$ the matrix $D_\varphi(\mathcal{P}_{110})$ is non degenerate so these solutions will be continued for $\epsilon \neq 0$ to provide multibreathers.

On the other hand, for the F_1, F_2 families of asymmetric vortices, $D_\varphi(\mathcal{P}_{110})$ is degenerate possessing one zero eigenvalue, reflecting the freedom of these solutions with respect to variations in φ. So, we cannot know at this level of perturbation theory if – or which of – these solutions can be continued to true multibreather solutions of the system.

In particular, for the configurations where the two families cross each other and correspond to the two symmetric vortices, i.e. $\boldsymbol{\varphi} = \pm\Phi^{(\rm sv)} \equiv \pm(\pi/2, \pi, -\pi/2)$, the matrix $D_\phi(\mathcal{P}_{101})$ reads

$$D_\varphi(\mathcal{P}_{101})|_{\Phi^{(\rm sv)}} = \begin{pmatrix} 0 & 0 & 0 \\ 0 & M'(\pi) & 0 \\ 0 & 0 & 0 \end{pmatrix} . \tag{16}$$

This means that its degeneracy is even higher since the dimension of its kernel is exactly two, i.e., given by the tangent directions to the two independent families in the vortex solutions. We will also attempt to numerically demonstrate this degeneracy in Section 5.

2.4.2. The $\mathcal{H}_{101}$ model.

The second example we consider is the $\mathscr{H}_{101}$ model, i.e., the model (2) with $k_2 = 0$ and $k_3 = 1$ which is described by the Hamiltonian

$$\begin{aligned} \mathscr{H}_{101} = &\sum_{j\in\mathbb{Z}} \left(\frac{1}{2}y_j^2 + \frac{1}{2}x_j^2 + \frac{1}{2}x_j^4\right) \\ &+ \frac{\epsilon}{2}\sum_{j\in\mathbb{Z}} \left[(x_{j+1}-x_j)^2 + (x_{j+3}-x_j)^2\right] . \end{aligned} \tag{17}$$

Such a system represents a first order approximation of a square NN lattice and a four-site multibreather solution of (17) can be thought of as representing a one-dimensional analogue of a four-site vortex for the two-dimensional square KG lattice and as it will be shown it constitutes a more degenerate case than the one of the $\mathscr{H}_{110}$ model (see Figures 4 and 5).

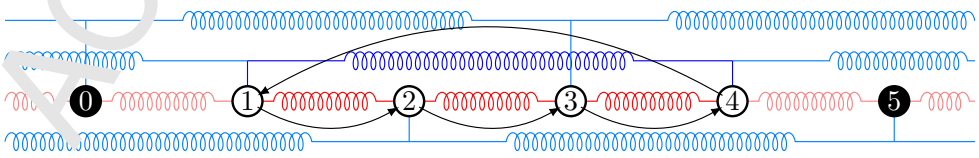

Figure 5: The one-dimensional model with first (red color) and third (blue color) neighbor interaction, whose 4-site MB corresponds at zero order with the 4-site MB of the square model. The dark version of the color indicates the interactions internal to the MB (corresponding to those of Figure 4). The numbers indicate the correspondence to the two-dimensional square model. Color online.

We consider again the persistence condition for this system, which are given by

$$\mathcal{P}_{101}(\boldsymbol{\varphi}) \equiv \begin{cases} M(\varphi_1) + M(\varphi_1+\varphi_2+\varphi_3) = 0 \\ M(\varphi_2) + M(\varphi_1+\varphi_2+\varphi_3) = 0 \\ M(\varphi_3) + M(\varphi_1+\varphi_2+\varphi_3) = 0 \end{cases} \tag{18}$$

where $M(\varphi)$ is given by (12). By using the symmetries of $M(\varphi)$ given in (13), it is easy to verify that Eqs. (18) and (12) admit three families of *asymmetric vortex* solutions

$$\begin{aligned} &F_1 : \boldsymbol{\varphi} = (\varphi, \varphi, \pi - \varphi) \ , \\ &F_2 : \boldsymbol{\varphi} = (\varphi, \pi - \varphi, \varphi) \ , \\ &F_3 : \boldsymbol{\varphi} = (\varphi, \pi - \varphi, \pi - \varphi) \ , \end{aligned} \tag{19}$$

in addition to the two isolated standard in/out-of phase solutions $F_{\rm iso} : \boldsymbol{\varphi} \in \big\{(0,0,0),\, (\pi,\pi,\pi)\big\}$.

Again, the rest of the standard configurations of this case are part of the F_1, F_2, F_3 families. These families are degenerate since the corresponding Jacobian $D_\varphi(\mathcal{P}_{101})$ possesses a zero eigenvalue, while the *symmetric vortex* solutions

$$\Phi^{(\rm sv)}_{101} \equiv \boldsymbol{\varphi} = \pm\Big(\frac{\pi}{2}, \frac{\pi}{2}, \frac{\pi}{2}\Big)$$

are fully degenerate, since $D_\varphi(\mathcal{P}_{101})$ equals the null matrix.

The latter can be seen both by a direct computation, or by observing that in these solutions we have three independent Kernel directions, one for each family passing through the solution. This degeneracy, which is higher of the one in the zigzag model, will be also numerically illustrated in Section 5.

2.4.3. Degeneracy in the corresponding dNLS models.

The same classification of degeneracies illustrated in the previous paragraphs naturally emerge also in the dNLS model (4) which can be derived from the corresponding KG model (2) by introducing complex variables $\psi_j = \frac{1}{\sqrt{2}}(x_j + iy_j)$ and keeping only terms resonant with respect to the periodic flow $\psi_j = e^{it}$. The Effective Hamiltonian Method clearly applies also to this class of models; however, the persistence condition (10) always leads to a set of trigonometric equations with $M(\varphi)$ given just by

$$M(\varphi) \equiv \sin(\varphi) \ . \tag{20}$$

For example, if we study continuation of discrete soliton corresponding to the set $S = \{1,2,3,4\}$ in the zigzag-dNLS

$$\begin{aligned} H_{110} = &\sum_j |\psi_j|^2 + \frac{3}{8}\sum_j |\psi_j|^4 \\ &+ \frac{\epsilon}{2}\sum_j \left[|\psi_{j+1} - \psi_j|^2 + |\psi_{j+3} - \psi_j|^2\right] \ , \end{aligned} \tag{21}$$

we note that condition (11) hold but with the function M given by (20). Thus, they become

$$\begin{cases} \sin(\varphi_1) + \sin(\varphi_1+\varphi_2) = 0 \\ \sin(\varphi_2) + \sin(\varphi_1+\varphi_2) + \sin(\varphi_3+\varphi_2) = 0 \\ \sin(\varphi_3) + \sin(\varphi_2+\varphi_3) = 0 \end{cases} \tag{22}$$

due to the rotational symmetry of the model (and of its discrete soliton solution); i.e. only the first mode of the Fourier expansion (8) contributes. In this case, it is straightforward to check that the persistence conditions (22) admit the two families of solutions given in (14), and that, apart from the other isolated and non-degenerate solutions, these are the only ones. Such a uniqueness-type of result is true also for the zigzag-KG problem, i.e., (11) and (12), in the limit of small enough action J^*: indeed, due to the exponentially fast decay of the coefficients $A_{2n-1}(J^*)$ in the Fourier expansion (8), in such a regime the higher harmonics in (8) are a very small perturbation of the first term $\cos(\theta)$, and one can observe that the solutions of the persistence condition (10) in the two models coincide. Indeed, it is clear that families of solutions of (22) are also solutions of (11). On the other hand, there are no other solutions for J^* small enough due to topological reasons: these families are non-degenerate in the transversal directions, hence there exists a neighborhood of them independent of the energy, where $\mathcal{P}$ vanishes only on the family itself. Outside this neighborhood, the persistence condition (22) is not satisfied, hence $\mathcal{P} \not\equiv 0$, and the same holds for a small enough perturbation (11). In other words, the solutions of (11) with $M(\varphi)$ given by (12) can be obtained, in the limit of small enough J^*, solving the system (22).

The same kind of correspondence can be noted between the KG model (17) and its corresponding dNLS system

$$\begin{aligned} H_{\rm ...} = &\sum_j |\psi_j|^2 + \frac{3}{8}\sum_j |\psi_j|^4 \\ &+ \frac{\epsilon}{2}\sum_j \left[|\psi_{j+1} - \psi_j|^2 + |\psi_{j+3} - \psi_j|^2\right] \ ; \end{aligned} \tag{23}$$

Indeed, if we study continuation of discrete solitons corresponding again to the set $S = \{1,2,3,4\}$ in the above model (23), we note that the conditions (18) hold but with M once again given by (20), i.e.,

$$\begin{cases} \sin(\varphi_1) + \sin(\varphi_1+\varphi_2+\varphi_3) = 0 \\ \sin(\varphi_2) + \sin(\varphi_1+\varphi_2+\varphi_3) = 0 \\ \sin(\varphi_3) + \sin(\varphi_1+\varphi_2+\varphi_3) = 0, \end{cases} \tag{24}$$

which has been the subject of a detailed investigation performed in [45]. Here again, in the limit of vanishing J^*, the families of solutions of (18) and (12) are independent on J^* and are the same for (24).

The exact correspondence of solutions between the persistence condition in KG models and in dNLS models is even more evident, if not obvious, in the other examples of degeneracies illustrated in the paragraph 2.3, being those cases totally degenerate (the whole resonant torus $\mathbb{T}^2$ is a solution of the persistence condition (10), also with (20)).

3. Abstract (non)existence results

As remarked in the final part of the previous section, in the regime of small energy and for some combination of excited sites S and linear interactions κ_i, solutions of the persistence condition (10) in the KG model, namely with $M(\varphi)$ given by (12), coincide with those in the corresponding dNLS model, where $M(\varphi)$ is given by (20).

Thus, *restricting to this class of degenerate scenarios*, we want to present two abstract statements allowing to rigorously derive results on the continuation of Multibreathers in the KG models from results on the continuation of discrete solitons in the "corresponding" dNLS models.

3.1. Setting and formulation

Let us consider the KG Hamiltonian (2) and its equations of motion

$$\ddot{x}_j = -x_j - x_j^3 + \epsilon(Lx)_j \ , \tag{25}$$

with the interaction terms encoded in

$$L := \Delta_1 + k_2\Delta_2 + k_3\Delta_3 \ ,$$
$$(\Delta_m x)_j := x_{j-m} - 2x_j + x_{j+m} \ .$$

We look for a periodic orbit with frequency γ; hence by introducing the time scaled variable $u_j(\tau) := x_j(t)$, where $\tau := \gamma t$, we rewrite (25) as

$$\gamma^2 u'' + u + u^3 - \epsilon L u = 0 \ . \tag{26}$$

By defining the operators

$$L_0 := \gamma^2\partial_\tau^2 + \mathbb{I} \ , \qquad L_\epsilon := L_0 - \epsilon L \ , \qquad N(u) := u^3 \ , \tag{27}$$

and by restricting to the Sobolev spaces of periodic functions $X_n := H^n\big([0,2\pi],\ell^2\big)$ (with $H^0 = L^2$), the equation (26) for a generic periodic orbit becomes

$$\mathscr{F}(\epsilon,u) := L_\epsilon u + N(u) = 0 \ , \tag{28}$$

with

$$\mathscr{F} : \mathbb{R}\times X_2 \to X_0 \ ,$$

where $\ell^2 = \ell^2(\mathbb{Z},\mathbb{R})$ and $X_{0,2}$ are endowed with the usual norms

$$\|u\|_{X_k}^2 := \sum_j \|u_j(t)\|_{H^k}^2 \ , \qquad k = 0,2 \ .$$

In the unperturbed case $\epsilon = 0$, we consider a periodic orbit $\bar{u}(\tau,\rho)$ which lies on the m-dimensional completely resonant torus (associated to $S = \{j_1,\dots,j_m\}$)

$$\bar{u}_l(\tau,\rho) := \begin{cases} 0 \ , & l \notin S \\ x(\tau+\theta_l) \ , & l \in S \end{cases} \ , \qquad x(\cdot) = \rho \tag{29}$$

We wish to understand which $\bar{u}(\tau,\rho)$, of small enough amplitude ρ, can be continued to periodic orbits for $\epsilon \neq 0$; thus we look for those $\bar{u}(\tau,\rho)$ which fulfill the following definition

Definition 3.1. *We say that $\bar{u}(\tau,\rho)$ can be continued to a solution of* (28) *if there exists $\rho^* > 0$ such that, for any $\rho < \rho^*$, there exist $\epsilon^*(\rho)$ and a function $u(\rho,\epsilon,\tau) \in X_2$ which solves for $|\epsilon| < \epsilon^*(\rho)$*

$$\mathscr{F}(\epsilon, u(\rho,\epsilon,\tau)) = 0 \ , \qquad u(\rho,0,\cdot) = \bar{u}(\tau,\rho) \ , \tag{30}$$

with γ kept fixed.

We introduce a special notation for standard MBs, whose existence is guaranteed by [42] independently of the choice of S: we denote by $\bar{u}_{\rm st}$ the unperturbed standard MBs

$$\bar{u}_{{\rm st},l}(\tau,\rho) := \begin{cases} 0 \ , & l \notin S \\ x(\tau+\theta_l) \ , & l \in S \ , \quad \theta_l - \theta_{j_1} \in \{0,\pi\} \end{cases} \ . \tag{31}$$

As already stressed at the beginning of this Section and in the Introduction, the main goal of the present paper is to provide either positive or negative answers to the existence of phase-shift solutions of (30), namely solutions which at $\epsilon = 0$ correspond to $\bar{u} \neq \bar{u}_{\rm st}$, by investigating the problem of continuation of phase-shift discrete solitons in the dNLS model (4).

In the dNLS context, when looking for periodic solutions of (4) with the form $\psi_j(t) = \phi_j(\epsilon)e^{i(1+\omega_0)t}$, we are led to study the stationary equation for the unknown spatial profile $\phi(\epsilon) \in \ell^2(\mathbb{Z};\mathbb{C})$

$$F(\phi,\epsilon) := -\omega_0\phi - \epsilon L\phi + \frac{3}{4}|\phi_l|^2\phi = 0 \ , \tag{32}$$

where ω_0 is the frequency detuning depending on the amplitude of the unperturbed solution $\phi(0)$. We introduce the unperturbed discrete soliton profile $v := \phi(0)$ of unit amplitude, which has the form

$$v_l = \begin{cases} 0 \ , & l \notin S \\ e^{-i\theta} \ , & l \in S \end{cases} \ , \qquad v : \mathbb{T}^m \to \ell^2(\mathbb{Z};\mathbb{C}) \ , \tag{33}$$

where $S = \{j_1,\dots,j_m\}$ is the same set of active sites chosen for the corresponding unperturbed Multibreather solution $\bar{u}(\tau,\rho)$. By its definition (33), v has to solve (32) with $\epsilon = 0$

$$\left(\frac{3}{4}|v_l|^2 - \omega_0\right) = 0 \ , \tag{34}$$

hence

$$|v_l| = \begin{cases} 1 \ , & l \in S \\ 0 \ , & l \notin S \end{cases} \ , \qquad \Rightarrow \qquad \omega_0 := \frac{3}{4} \ . \tag{35}$$

We consider a solution v of the uncoupled problem and ask for its continuation for $\epsilon \neq 0$; we thus look for a correction $w(\epsilon)$ around v, namely

$$w(v,\epsilon) := \phi(\epsilon) - v \ , \qquad \text{with} \quad w(v,0) = 0 \ ,$$

that is continuous in ϵ and such that $\phi(\epsilon)$ solves (32).

Inserting the above definition, and exploiting that v is a solution for $\epsilon = 0$, equation (32) takes the form

$$F(v;w,\epsilon) = 0 \ , \quad \text{with} \quad F(v;0,0) = 0 \ . \tag{36}$$

The usual strategy to solve (36) is to probe the applicability of the implicit function theorem, by considering the linear operator

$$\Lambda := (D_w F)\,(v;0,0) \ . \tag{37}$$

It is not difficult to check that Λ has a m-dimensional kernel which inhibits the application of the implicit function theorem; this justifies the need of a Lyapunov-Schmidt decomposition. By following the same strategy of [45], we introduce the splitting $w = k + h$ where

$$k \in K := \mathrm{Ker}(\Lambda) \simeq \mathbb{R}^m \ , \qquad h \in H := \mathrm{Range}(\Lambda) \simeq K^\perp \ ,$$

so that equation (36) is equivalent to the system

$$\begin{cases} F_H(v;k+h,\epsilon) = 0 \\ F_K(v;k+h,\epsilon) = 0 \end{cases} \ ,$$

where the subscripts H and K denote the corresponding projections Π_H and Π_K over $\mathrm{Range}(\Lambda)$ and $\mathrm{Ker}(\Lambda)$, respectively.

The Range equation $F_H = 0$ can be solved locally by the implicit function theorem and provides

$$h = h(v; k, \epsilon) \ ; \tag{38}$$

inserting (38) into $F_K = 0$ we get the **bifurcation equation**, redefining F_K as

$$0 = F_K(v; k, \epsilon) := F_K(v; k + h(v, k, \epsilon), \epsilon) \ , \tag{39}$$

where now

$$F_K : \mathbb{R}^m \times \mathbb{R} \to \mathbb{R}^m \ ,$$

is defined once given the unperturbed reference solution v and is analytic in ϵ. We here recall that $v \in H$ and that

$$F_K(v; k, 0) = 0 \ , \qquad \forall v \in H \ , \qquad \forall k \in K \ ;$$

indeed, geometrically speaking, for any tangential displacement k there exists a unique transversal displacement $h(k)$ such that $\phi = v + w$ is a solution of the equation (32) with $\epsilon = 0$. As a consequence, F_K is at least of order $\mathcal{O}(\epsilon)$, namely

$$F_K(v; k, \epsilon) = \epsilon P(v; k, \epsilon) \ , \tag{40}$$

and (39) becomes

$$P(v; k, \epsilon) = 0 \ . \tag{41}$$

For a given $v \in H$, we are interested in a small correction $k(\epsilon) \in K$, continuous in ϵ for small enough $|\epsilon| \ll 1$, such that $P(v; k(\epsilon), \epsilon) = 0$. We start with some definitions:

Definition 3.2. *We denote by v^* any solution of*

$$P(v; 0, 0) = 0 \ , \tag{42}$$

and by p an integer such that

$$dim(Ker(D_k P(v^*; 0, 0))) = p + 1 \ .$$

Then

1. *v^* is said* non-degenerate *if $p = 0$;*
2. *a solution $\phi = v^* + w(v^*, \epsilon)$ of (32) is said to be* non-degenerate *if v^* is non-degenerate;*
3. *v^* is said* p-degenerate *if $1 \leqslant p \leqslant m - 1$.*

In more geometrical terms, nondegeneracy means that the only kernel direction of $D_k P(v^*, 0, 0)$ is given by the velocity of the unperturbed orbit, that in the case of discrete solitons coincides with the gauge vector field. On the other hand, v^* is said to be degenerate if there exist at least two independent Kernel directions for $D_k P(v^*; 0, 0)$. As in the examples illustrated in the previous Section for the KG model, degeneracy typically arises when solutions of (42) appear in $d+1$ families $v^*(\theta_{j_1}, \varphi)$, with

$$\varphi = (\varphi_1, \dots, \varphi_d) \ , \qquad 1 \leqslant d \leqslant m - 1$$

being a local parametrization of the subtorus $\mathbb{T}^d \subset \mathbb{T}^m$. In general, we expect that a given v^* on such a family is d-degenerate, with the Kernel of $D_k P(v^*; 0, 0)$ being given by the tangent directions $\partial_{\theta_{j_1}} v^*$ and $\partial_{\varphi_l} v^*$. However, families can intersect each other, like in the four-sites examples of Section 2.4, where either two (see (14)) or three families (see (19)) intersect in vortex configurations: hence, transversal intersections are even more degenerate and we can expect p-degeneracy with $d < p \leqslant m-1$.

Equation (42) selects those unperturbed solutions v^* which might survive to the breaking of the resonant torus due to the effect of the perturbation. By introducing the resonant set of angles (9), it turns out that v can be parametrized by $m-1$ slow angles φ_l and one fast angle θ_{j_1}, namely $v(\theta_{j_1}, \varphi_1, \dots, \varphi_{m-1})$. The next Lemma provides the connection between the persistence condition (10) emerging in the framework of averaging theory, and equation (42), which naturally arises as a necessary condition to solve the bifurcation equation.

Lemma 3.1. *The above condition* (42) *is equivalent (in the sense of coincidence of solutions) to the* persistence condition (10) *with $M(\varphi)$ given by* (20).

Proof: We propose two different proofs. The most direct one, is based on the explicit expression of $P(v; 0, 0)$, since from a straightforward calculation one gets

$$P(v; 0, 0) = \Pi_K L v = 0 \ .$$

Once the basis of K is given, projections of Lv over vectors belonging to K are performed using the complex inner scalar product $a \cdot b = \sum_j \Re(a_j \bar{b}_j)$, where a basis $\{e_l\}_{l=1,\dots,m}$ for K is given by

$$e_1 = \partial_{\theta_{j_1}} v^*(\theta_{j_1}, \varphi) \ , \qquad e_l = \partial_{\varphi_l} v^*(\theta_{j_1}, \varphi) \ .$$

Explicit calculations show the equivalence between the two systems of trigonometric equations, namely (10) and (42). As a second proof, we recall that the equivalence of the two systems is a consequence of the variational Lyapunov-Schmidt decomposition of (32) (see [5], Section 1.2), according to which the bifurcation equation (41) can be obtained differentiating with respect to the kernel variables k the restriction to $\phi = v + k + w(v; k, \epsilon)$ of the dNLS functional $S(\phi, \bar{\phi}, \epsilon)$ associated to (32). Expanding S in powers of ϵ, namely $S = S_0 + \epsilon S_1$, it turns out that the system (42) is equivalent to finding critical points of $S_1(v)$ (as already shown by Kapitula in [21]; see also applications in [22, 24]). □

Now we can move to claim the two following statements. The first one allows to derive, in a suitable regime of small energy $\mathcal{H}(x, y) = E$ and coupling ϵ, an existence and approximation result for a solution $u(\rho, \epsilon, \tau)$ of (26), from the existence of a non-degenerate dNLS discrete soliton $\phi(\epsilon)$ which is solution of (32):

Theorem 3.1. *Let $\phi(\epsilon)$ be a non-degenerate ϵ-family of solutions for*

$$-\omega_0 \phi - \epsilon L \phi + \frac{3}{4} |\phi|^2 \phi = 0$$

with $\phi(0)$ given by (33)*, and let*

$$\mathsf{v}(\epsilon, \tau) := \frac{\rho}{2} \left[e^{-i\tau} \phi(\epsilon) + c.c. \right] \tag{43}$$

be the corresponding real solution of amplitude ρ. Then, there exist E^* and ϵ^* such that, for $0 < E < E^*$ and $\epsilon < E\, \epsilon^*$, there exist a constant C_1 and a unique non-degenerate two parameter family $u(\rho, \epsilon, \tau)$, solutions of (28)*, which fulfills*

$$u(\rho, \epsilon, \cdot) = \mathsf{v}(\epsilon, \cdot) + \mathcal{O}(\rho^3) \ . \tag{44}$$

A couple of remarks are in order:

- The true solution and its approximation are of order $\mathcal{O}(\rho) \sim \mathcal{O}(\sqrt{E})$, thus the correction, being of order $\mathcal{O}(\rho^3) = \mathcal{O}(E^{3/2})$, is a small perturbation. We stress that two different kind of remainders contribute to the $\mathcal{O}(\rho^3)$ correction. The first one is due to the fact that, in the small amplitude regime, higher harmonics of the time-Fourier decomposition of the periodic solution $u(\rho, \epsilon, \tau)$ are a perturbation of the first harmonic $\rho e^{-i\tau}$ (see Step A of Section 3.3 for details). The second one is instead due to the fact that $\phi(\epsilon)$ represents only a leading order approximation of the Fourier coefficient of $e^{-i\tau}$ (see Step C of of Section 3.3 for details).
- since the expansion (44) holds even at $\epsilon = 0$, it means that the nondegeneracy of an unperturbed discrete soliton $\phi(0)$ guarantees, provided ρ small enough, the existence of a "corresponding" unperturbed solution $\bar{u}(\rho, \tau)$, close to $\rho\phi(0)$, which can be uniquely continued to $u(\rho, \epsilon, \tau)$.

The second statement, dealing with degenerate scenarios, holds true under the following more restrictive assumption:

Assumption 3.1 (H0). *There exists E^* such that, for $0 < E < E^*$ degenerate solutions of* (10) *with* (12) *and with* (20) *coincide.*

We are going to provide a criterion to derive, for the KG model, the nonexistence of degenerate phase-shift (i.e. those which are not continuations of $\bar{u}_{st}$) Multibreathers, on the base of the nonexistence of degenerate phase-shift discrete solitons of the dNLS; we have to first recall that (42) always admits standard configurations

$$v^*_{\mathrm{st},l} := \begin{cases} 0 \ , & l \notin S \\ e^{-i\theta_l} \ , & l \in S \ , \qquad \theta_l - \theta_{j_1} \in \{0, \pi\} \end{cases} \ , \tag{45}$$

independently of their degeneracy.

Theorem 3.2. *Assume that for any p-degenerate v^*, with any $1 \leqslant p \leqslant m-1$ and different from the standard ones v^*_{st}, the following conditions hold true*

$$\textit{(H1)} \qquad rk(D_k P(v^*; 0, 0)) = m - p - 1 \ , \tag{46}$$

$$\textit{(H2)} \qquad \partial_\epsilon P(v^*; 0, 0) \not\equiv 0 \ , \tag{47}$$

$$\textit{(H3)} \qquad \partial_\epsilon P(v^*; 0, 0) \notin Range(D_k P(v^*; 0, 0)) \ . \tag{48}$$

Then, in the limit of vanishing energy E, only $\bar{u}_{st}$ can be continued at $\epsilon \neq 0$ to Multibreathers solutions $u(\tau, \rho, \epsilon)$ of (26).

Here we have to stress some facts:

- It follows by direct calculations that

  $$\partial_\epsilon P(v^*_{st}; 0, 0) \equiv 0 \ ,$$

  as expected from the fact that real discrete solitons $\phi \in \ell^2(\mathbb{Z}, \mathbb{R})$ always exist in models (32).
- Assumption (H3) is equivalent to assuming the algebraic and geometric multiplicity of the zero eigenvalue of $D_k P(v^*; 0, 0)$ to be equal, which provides

  $$\mathrm{rk}(D_k P(v^*; 0, 0)) + \dim(\mathrm{Ker}(D_k P(v^*; 0, 0))) = m \ .$$

  This allows to perform a second Lyapunov-Schmidt decomposition on the equation (41).
- Theorem 3.2 does not exclude that phase-shift Multibreathers might appear for large enough ϵ. It only claims that there do not exist continuous (in ϵ) branches starting at $\epsilon = 0$ from degenerate solutions $\bar{u} \neq \bar{u}_{\mathrm{st}}$.

In cases of complete degeneracy, when the persistence condition (42) is trivially satisfied

$$P(v; 0, 0) \equiv 0 \ , \qquad \forall v \in U \ ,$$

the above statement simplifies. Indeed, in this case, for any v we have

$$\mathrm{Range}(D_k P(v; 0, 0)) = \{0\} \ ,$$

hence condition (H2) implies (H3) and we have the following

Corollary 3.1. *Assume that $P(v; 0, 0) \equiv 0$ for all v defined in* (33) *and that for any $v \neq v_{st}$ the following condition is fulfilled*

$$\partial_\epsilon P(v; 0, 0) \not\equiv 0 \ , \tag{49}$$

Then the same as in Theorem 3.2 holds true.

3.2 A roadmap of the proof

We recall that the problem (26) has been partially solved in [28] by restricting to time-reversible solutions $u(-\tau) = u(\tau)$; i.e., by considering only standard phase-differences $\varphi_l = \{0, \pi\}$ for all $l \in S$. Indeed, with this strategy the problem reduces to non-degenerate critical points where the implicit function theorem can be applied, like in the averaging approach of [1, 31, 32]. In the case of other phase-differences, namely phase-shift multibreathers we consider here, it is not possible to make such a restriction, which ensures invertibility of the linearized operator $\mathscr{F}_u(0, \bar{u})$ on the subspace of even periodic solutions. In other words, in our case, the approximate solution $\bar{u}$ is a degenerate critical point; thus a small perturbation may in principle destroy the solution. In order to geometrically see that the linearized operator $\mathscr{F}_u(0, \bar{u})$ has a non-trivial Kernel, observe that a small displacement on the m-dimensional torus from a given unperturbed periodic solution, leads to a new unperturbed periodic solution with the same frequency.

First, notice that

$$\mathscr{F}_u(0, \bar{u})[\zeta] = \begin{cases} L_0 \zeta_l & l \notin S \ , \\ L_0 \zeta_l + 3\bar{u}^2(\tau)_l \zeta_l & l \in S \ . \end{cases}$$

The non-resonant condition $j\gamma \neq \pm 1$, which coincides with (NR) of the Effective Hamiltonian Method, allows to invert L_0 on the space of 2π-periodic functions. On the other hand, differentiating the nonlinear oscillation equation w.r.t. both τ and the energy E, one sees that

$$\mathrm{Ker}\Big(\mathscr{F}_u(0, \bar{u})\Big|_S\Big) = \mathsf{Span}\{x'(\tau + \theta_l), \tau \frac{\partial \gamma}{\partial E} x'(\tau + \theta_l)\};$$

as a consequence, the non-degeneracy condition of the frequency $\frac{\partial \gamma}{\partial E} \neq 0$, which in our case is equivalent to (ND-K) of the Effective Hamiltonian Method, guarantees that only the time derivatives $x'(\tau + \theta_l)$ are 2π-periodic solutions. Thus the differential $\mathscr{F}_u(0, \bar{u})$ has a m-dimensional Kernel

$$\mathrm{Ker}(\mathscr{F}_u(0, \bar{u})) = \mathsf{Span}\{f_l(\tau)\}_{l \in S} \ ,$$

generated by the velocities of the nonlinear oscillations

$$f_l = \begin{cases} 0 \ , & l \notin S \\ x'(\tau+\theta_l) \ , & l \in S \end{cases} \ .$$

For the above reason an implicit function theorem cannot be applied (unless, as in [43], we restrict to $\varphi_l \in \{0,\pi\}$, which allows to do without (ND-P)), and a Lyapunov-Schmidt decomposition represents a natural approach to the problem.

The proofs start exactly with a first Lyapunov-Schmidt decomposition, based on the time-Fourier expansion of the periodic solution u of (26). This is a classical approach which allows to decompose the solution into a leading order "monochromatic" wave, say $\mathsf{v}(\tau)$, and a smaller correction, say $\mathsf{w}(\tau) = \mathcal{O}(\mathsf{v}^3)$, given by all the higher harmonics. The coefficients of the leading term $\mathsf{v}(\tau)$ can be collected into a complex variable $\phi \in \ell^2(\mathbb{Z};\mathbb{C})$ which has to satisfy a *dNLS-type stationary equation*; this equation for the unknown ϕ turns out to be a perturbation of order $\mathcal{O}(\rho^2)$ (from here on the squared-amplitude ρ^2 plays the role of a second small parameter) of the dNLS equation (32). Thus, this first part of the proof, developed in Step A, translates the problem of the existence of a periodic orbit for (26) into the existence of of a discrete soliton ϕ, satisfying a perturbation of (32). The second parts of the proofs, Step B, consist of studying the existence of phase-shift discrete solitons in the perturbed dNLS stationary equation previously obtained: this is done with a second Lyapunov-Schimidt decomposition, which translates the original problem into the study of a *bifurcation equation* which is a perturbation of order $\mathcal{O}(\rho^2)$ of the dNLS bifurcation equation (41). In the third and last part of the proofs, Step C, we exploit the smallness of the "energy" ρ^2, and the smoothness with respect to this small parameter of the various equations involved, in order to transfer existence and nonexistence criteria more straightforwardly formulated and verified at the level of the standard dNLS equation (32), to the perturbed bifurcation equation obtained in Step B, hence producing the statements claimed in Theorems 3.1 and 3.2.

3.3. Proofs

Step A: From the KG to the perturbed dNLS

We start by showing that the problem of searching time-periodic solutions u of (26) with fixed frequency γ, is equivalent to finding the profile ϕ of a discrete soliton solution for a dNLS-like model.

Proposition 3.1. *There exists a function* $\mathscr{R}_\rho$

$$\mathscr{R}_\rho(\phi,\bar\phi,\rho^2,\epsilon) : \ell^2(\mathbb{Z};\mathbb{C}) \times \mathbb{R} \times \mathbb{R} \to \ell^2(\mathbb{Z};\mathbb{C}) \ ,$$

fulfilling

$$\left\|\mathscr{R}_\rho(\phi,\bar\phi,\rho^2,\epsilon)\right\|_{\ell^2} = \mathcal{O}(\|\phi\|_{\ell^2}^5) \ ,$$

and a constant ω_ρ, *fulfilling*

$$\omega_\rho = \frac{3}{4} + \mathcal{O}(\rho^2) \ , \tag{50}$$

such that equation (26) *is equivalent to*

$$-\omega_\rho\phi - \epsilon L\phi + \frac{3}{4}|\phi|^2\phi + \rho^2\mathscr{R}_\rho(\phi,\bar\phi,\rho^2,\epsilon) = 0 \ . \tag{51}$$

Proof:

We consider (26) and we introduce the time-Fourier expansion for the solution of the uncoupled anharmonic oscillator $x(\tau)$ in (6)

$$x(\tau) = \sum_{k\geqslant 1} a_k \cos(k\tau) \ , \tag{52}$$

where the average $a_0 = 0$ because of the symmetry of the potential V. Then, from (29), we get

$$\bar u_l(\tau,\rho) = \begin{cases} 0 & l \notin S \\ \sum_{k\geqslant 1} a_{2k-1}\cos[(2k-1)(\tau+\theta_l)] & l \in S \end{cases} \ ,$$

thus, for any $l \in S$, we can write

$$\bar u_l = \sum_{k\geqslant 1} a_{2k-1}\Big(\cos[(2k-1)\theta_l]\cos[(2k-1)\tau] - \sin[(2k-1)\theta_l]\sin[(2k-1)\tau]\Big) \ .$$

Let us now introduce the Fourier base

$$e_k(\tau) = \begin{cases} \cos[(2k-1)\tau] & k > 0 \\ -\sin[(2k+1)\tau] & k < 0 \end{cases} \ ; \tag{53}$$

we can decompose $u \in \ell^2(\mathbb{R})$ in its Fourier components

$$u(\tau,\rho) = \sum_{k\in\mathbb{Z}\setminus\{0\}} u_k(\rho)e_k(\tau) \ , \tag{54}$$

and introduce the Lyapunov-Schmidt decomposition[1] which splits the first harmonics from the rest of the Fourier expansion

$$u = \mathsf{v} + \mathsf{w} \ , \qquad \mathsf{v} := u_{-1}e_{-1}(\tau) + u_1 e_1(\tau) \ ; \tag{55}$$

in other words v solves $\left(\partial_\tau^2 + \mathbb{I}\right)\mathsf{v} = 0$. We define

$$V_2 := \mathsf{Span}\{e_1, e_{-1}\} = \ker\left(\partial_\tau^2 + \mathbb{I}\right) \ , \quad W_2 := V_2^{\complement} \ , \tag{56}$$

so that $\mathsf{v} \in V_2$. If we consider the unperturbed solution $\bar u = \bar{\mathsf{v}} + \bar{\mathsf{w}}$ in (29), we have for any component $l \in S$

$$\bar u_l = \sum_{k\in\mathbb{Z}} \bar u_{l,k} e_k(\tau) \ , \quad \bar u_{l,k} = \begin{cases} a_{2k-1}\cos[(2k-1)\theta_l] & k > 0 \\ 0 & k = 0 \\ a_{2k+1}\sin[(2k+1)\theta_l] & k < 0 \end{cases} \ ,$$

thus we get

$$\bar{\mathsf{v}}_l = a_1\cos(\theta_l)e_1(\tau) - a_1\sin(\theta_l)e_{-1}(\tau) \ . \tag{57}$$

We introduce the detuning ω

$$\omega := \gamma^2 - 1 \ , \tag{58}$$

so that we can rewrite $\gamma^2 = 1 + \omega$. Indeed, as will be shown at the end of the proof, in the small energy regime, the frequency γ is close to one, and its displacement ω is of order $\mathcal{O}(\rho^2)$. The equation (26) thus reads

$$\mathscr{F}(\epsilon,\mathsf{v},\mathsf{w}) = L_\epsilon\mathsf{w} - \omega\mathsf{v} - \epsilon L\mathsf{v} + N(\mathsf{v}+\mathsf{w}) = 0 \ . \tag{59}$$

[1] Please notice the use of the sans serif font for the present decomposition variables: v and w. Letters v and w, with the usual font, have a different meaning.

When we project (59) on the Range $W_0 \subset X_0$ of $\partial_\tau^2 + \mathbb{I}$, and its complement V_0, we get[2]

$$\begin{cases} \Pi_W \mathscr{F}(\epsilon, \mathsf{v}, \mathsf{w}) = L_\epsilon \mathsf{w} + \Pi_W N(\mathsf{v}+\mathsf{w}) = 0 & (R) \\ \Pi_V \mathscr{F}(\epsilon, \mathsf{v}, \mathsf{w}) = -\omega \mathsf{v} - \epsilon L \mathsf{v} + \Pi_V N(\mathsf{v}+\mathsf{w}) = 0 & (K) \end{cases} . \tag{60}$$

The Range equation (R), written as $\mathsf{w} = -L_\epsilon^{-1}\Pi_W N(\mathsf{v}+\mathsf{w})$, can be locally solved in terms of $\mathsf{w}(\mathsf{v}, \epsilon)$ by Implicit Function Theorem; moreover, the implicit solution $\mathsf{w}(\mathsf{v}, \epsilon)$ can be explicitly approximated by $\tilde{\mathsf{w}}(\mathsf{v}, \epsilon) = \mathcal{O}(\|\mathsf{v}\|^3_{X_2})$,

$$\tilde{\mathsf{w}}(\mathsf{v}, \epsilon) := -L_\epsilon^{-1}\Pi_W N(\mathsf{v}) , \qquad \|\mathsf{w} - \tilde{\mathsf{w}}\|_{X_2} \leqslant C \|\mathsf{v}\|^5_{X_2} . \tag{61}$$

We move now to the Kernel equation (K). Because of (61), we Taylor-expand in v

$$\begin{aligned} \Pi_V\big((\mathsf{v}+\mathsf{w}(\mathsf{v},\epsilon))^3\big) &= \Pi_V(\mathsf{v}^3) + \mathscr{R}(\mathsf{v}, \epsilon) \\ \mathscr{R}(\mathsf{v}, \epsilon) &:= \Pi_V\big((\mathsf{v}+\mathsf{w}(\mathsf{v},\epsilon))^3\big) - \Pi_V(\mathsf{v}^3) = \\ &= \mathcal{O}(\|\mathsf{v}\|^5_{X_2}). \end{aligned} \tag{62}$$

We compute explicitly the Kernel projection of the leading term of the nonlinear part. First we have, by definition

$$\begin{aligned} \Pi_V(\mathsf{v}^3) = &\left(\frac{1}{2\pi}\int_0^{2\pi} \mathsf{v}^3(\tau)\cos(\tau)d\tau\right)e_1 + \\ &+ \left(\frac{1}{2\pi}\int_0^{2\pi} \mathsf{v}^3(\tau)\sin(\tau)d\tau\right)e_{-1} , \end{aligned}$$

and since, omitting the τ dependence, we have

$$\mathsf{v}^3 = u_1^3 e_1^3 + 3u_1^2 u_{-1} e_1^2 e_{-1} + u_{-1}^3 e_{-1}^3 + 3u_1 u_{-1}^2 e_1 e_{-1}^2 ,$$

trigonometric formulas give immediately

$$\begin{aligned} \Pi_V(\mathsf{v}^3) &= \frac{3}{4}\big((u_1^2+u_{-1}^2)u_1\cos(\tau) + (u_1^2+u_{-1}^2)u_{-1}\sin(\tau)\big) \\ &= \frac{3}{4}(u_1^2+u_{-1}^2)\mathsf{v} . \end{aligned} \tag{63}$$

By using (62) and the above, the Kernel equation reads

$$-\omega\mathsf{v} - \epsilon L\mathsf{v} + \frac{3}{4}(u_1^2+u_{-1}^2)\mathsf{v} + \mathscr{R}(\mathsf{v},\epsilon) = 0 \tag{64}$$

The Kernel equation, due to its dimension (v is a two-dimensional vector of sequences), is equivalent to the system

$$\begin{aligned} -\omega u_1 - \epsilon L u_1 + \frac{3}{4}(u_1^2+u_{-1}^2)u_1 + \mathscr{R}(\mathsf{v},\epsilon)\cdot e_1 = 0 \\ -\omega u_{-1} - \epsilon L u_{-1} + \frac{3}{4}(u_1^2+u_{-1}^2)u_{-1} + \mathscr{R}(\mathsf{v},\epsilon)\cdot e_{-1} = 0 \end{aligned} . \tag{65}$$

Multiplying the second of the above by the imaginary part i and summing with the first, equation (64) takes the compact form in terms of the complex variable ϕ

$$-\omega\phi - \epsilon L\phi + \frac{3}{4}\phi|\phi|^2 + \mathscr{R}(\phi, \bar{\phi}, \epsilon) = 0 , \qquad \phi := u_1 + iu_{-1} , \tag{66}$$

where we used again the letter $\mathscr{R}$ to denote the corresponding term of (64)

$$\begin{aligned} \mathscr{R}(\phi, \bar{\phi}, \epsilon) = &\frac{1}{2\pi}\int_0^{2\pi}\left[(\mathsf{v}+\mathsf{w}(\mathsf{v},\epsilon))^3 - \mathsf{v}^3\right]\cos(\tau)d\tau + \\ &+ \frac{i}{2\pi}\int_0^{2\pi}\left[(\mathsf{v}+\mathsf{w}(\mathsf{v},\epsilon))^3 - \mathsf{v}^3\right]\sin(\tau)d\tau ; \\ \mathsf{v} = &\frac{1}{2}\Big(\phi e^{-i\tau} + c.c.\Big) . \end{aligned} \tag{67}$$

It turns out that in the small energy regime (i.e., for ρ small enough) the term $\mathscr{R}(\phi, \epsilon)$ in equation (66) can be treated as a perturbation of order $\mathcal{O}(\rho^2)$ of the dNLS stationary problem

$$-\omega\phi - \epsilon L\phi + \frac{3}{4}\phi|\phi|^2 = 0 . \tag{68}$$

Indeed, introducing the following ρ-scaling

$$\phi =: \rho\tilde{\phi} , \qquad \epsilon =: \rho^2\tilde{\epsilon} , \qquad \omega =: \rho^2\omega_\rho , \tag{69}$$

and immediately *dropping the tildes*, equation (66) corresponds to (51). In order to show the order of magnitude, recall that from the definition of $\mathscr{R}$ in (62) and from the definition of v in (55) we have

$$\|\mathscr{R}(\mathsf{v})\| = \mathcal{O}(\|\mathsf{v}\|^5_{X_2}) = \mathcal{O}(\|\phi\|^5_{\ell^2}) ,$$

which provides a prefactor ρ^2 in front of $\mathscr{R}_\rho$ (after dividing by ρ^3) and the estimate on $\mathscr{R}_\rho$. The additional dependence of $\mathscr{R}_\rho$ on ρ^2 is a consequence of the scaling in the amplitude applied to the cubic nonlinearity, which is preserved along the Lyapunov-Schmidt decomposition.

The dependence of ω_ρ on ρ^2 is also a consequence of the same scaling, which can be revealed with a standard (Poincaré-Lindtsedt) perturbation scheme on the Duffing Oscillator (6). For example, one can rescale $x(\tau)$ by ρ to get

$$\gamma^2 x'' + x + \rho^2 x^3 = 0 , \tag{70}$$

and then Taylor-expand in ρ^2 both the solution

$$x = x_0 + \rho^2 x_2 + h.o.t.$$

and the squared frequency

$$\gamma^2 = 1 + \rho^2\omega_0 + \mathcal{O}(\rho^4) .$$

At order $\mathcal{O}(\rho^2)$ one gets the forced harmonic oscillator

$$x_2'' + x_2 = -x_0^3 - \omega_0 x_0'' ;$$

in order to avoid secular terms in the solution x_2, we need $\omega_0 = \frac{3}{4}$, from which the asymptotic behaviour of ω_ρ. □

Remark 3.1. *Notice that at $\rho = 0$, the constant ω_ρ turns out to be the quantity ω_0 in the stationary equation* (32)

$$\omega_\rho\Big|_{\rho=0} = \frac{3}{4} = \omega_0 .$$

Remark 3.2. *In Equation* (51)*, and in the rest of the present Section, ϵ won't be anymore the original KG coupling (remember we are dropping the tildes of the scaling* (69)*), but it will represent the coupling of the (perturbed) dNLS equation* (51) *associated to the original KG equation* (26)*. Due to the scaling introduced in* (69)*, it turns out to be the original coupling ϵ divided by the squared amplitude ρ^2.*

[2] For an easier notation we drop the zero subscript in the projectors $\Pi_V \equiv \Pi_{V_0}$ and $\Pi_W \equiv \Pi_{W_0}$.

Proposition 3.2. *Equation* (51) *is invariant under the gauge-action and under conjugation. Moreover, there exists a Hamiltonian function* $S_\rho(\phi,\bar\phi,\rho^2,\epsilon)$ *such that*

$$\nabla_{\bar\phi} S_\rho = -\omega_\rho\phi - \epsilon L\phi + \frac{3}{4}|\phi|^2\phi + \rho^2\mathscr{R}_\rho(\phi,\bar\phi,\rho^2,\epsilon)$$

Proof: We here exploited the sketched procedure of the variational Lyapunov-Schmidt decomposition in [5]. Periodic orbits with fixed period are critical points of the action

$$S(u) := \frac{1}{T}\int_0^T \mathcal{L}(u,u')dt \ , \tag{71}$$

where $\mathcal{L}$ is the Lagrangian giving the evolution equations (26) for u. The Kernel equation (66) preserves the variational nature of the problem (71), hence it is the differential of the reduced action

$$-\omega\mathsf{v} - \epsilon L\mathsf{v} + \Pi_V(\mathsf{v}+w(\mathsf{v},\epsilon))^3 = D_{\mathsf{v}}S(\mathsf{v}+\mathsf{w}(\mathsf{v},\epsilon)) \ .$$

If we pass to complex variables ϕ introduced in (66), this means that

$$-\omega\phi - \epsilon L\phi + \frac{3}{4}\phi|\phi|^2 + \mathscr{R}(\phi,\bar\phi,\epsilon) = D_{\bar\phi}S(\phi,\bar\phi) \ ,$$

where

$$S(\phi,\bar\phi) = \frac{1}{2\pi}\int_0^{2\pi}\mathcal{L}\Big(\Big(\frac{1}{2}\phi e^{-i\tau}+c.c\Big),\Big(\frac{1}{2}\phi e^{-i\tau}+c.c.\Big)'\Big)d\tau \ . \tag{72}$$

The Hamiltonian S_ρ is obtained scaling the above S with the scale transformation (69). The gauge invariance of S_ρ is understood observing that the gauge action is the periodic flow defining the Kernel space. A direct computation shows this explicitly on S

$$S(e^{i\theta}\phi, e^{-i\theta}\bar\phi) = S(\phi,\bar\phi) \ .$$

The invariance under conjugation can be obtained in the same way, exploiting also the even parity w.r.t. the velocity u'. □

Step B: Existence and nonexistence of degenerate discrete solitons in the perturbed dNLS model

At $\epsilon = 0$, we denote by v_ρ the unperturbed solution of (51), corresponding to the Kernel projection $\bar{\mathsf{v}}$ in (57) scaled by ρ

$$v_{\rho,l} = \begin{cases} 0 \ , & l\notin S \\ \frac{a_1}{\rho}e^{-i\theta_l} \ , & l\in S \ ; \end{cases} \tag{73}$$

the unperturbed solution v_ρ has amplitude $a_1/\rho = \mathcal{O}(1)$ and is linked to ω_ρ by the relation

$$\omega_\rho = \frac{3}{4}|v_\rho|^2 + \rho^2\frac{\mathscr{R}_\rho(v_\rho,\rho^2,0)}{v_\rho} \ .$$

It is clear that, as $\rho\to 0$, one has

$$v_\rho \to v \ , \qquad \omega_\rho \to \omega_0 \ .$$

Once we focus on a particular solution v_ρ of the unperturbed problem, we ask for its continuation for $\epsilon\neq 0$; we thus introduce a small displacement w from v_ρ, so that ϕ in (51) can be decomposed in

$$\phi = v_\rho + w \ ,$$

and we look for a correction $w = w_\rho(v_\rho,\epsilon)$ of v_ρ, that is continuous in ϵ, namely

$$w_\rho(v_\rho,\epsilon) := \phi_\rho(\epsilon) - v_\rho \ , \qquad \text{with} \qquad w_\rho(v_\rho,0) = 0 \ ,$$

so that $\phi = \phi_\rho(\epsilon)$ solves (51). Inserting the above decomposition of ϕ, the Kernel equation (51) takes the form

$$\mathcal{F}(v_\rho; w, \rho^2, \epsilon) = 0 \ , \tag{74}$$

where the explicit dependence on ρ^2 is due to ω_ρ and to the remainder $\rho^2\mathscr{R}_\rho(v_\rho+w,\rho^2,\epsilon)$. The usual strategy to solve (74) is to proceed with a further Lyapunov-Schmidt decomposition (for the same reasons explained in Section 3.1), at the level of the displacement w

$$w = k_\rho + h_\rho \ , \quad k_\rho\in\mathrm{Ker}(\Lambda_\rho) \ , \quad h_\rho\in\mathrm{Range}(\Lambda_\rho) \ ,$$

where

$$\Lambda_\rho := (D_w\mathcal{F})(v_\rho;0,\rho^2,0) \ . \tag{75}$$

The equation (85) then becomes

$$\begin{cases} \mathcal{F}_H(v_\rho, k_\rho+h_\rho, \rho^2,\epsilon) = 0 \\ \mathcal{F}_K(v_\rho, k_\rho+h_\rho, \rho^2,\epsilon) = 0 \end{cases} ,$$

where the subscripts H and K denote the corresponding projections over $\mathrm{Range}(\Lambda_\rho)$ and $\mathrm{Ker}(\Lambda_\rho)$, respectively. The Range equation $\mathcal{F}_H = 0$ can be solved locally by the implicit function theorem and provides

$$h_\rho = h_\rho(v_\rho; k_\rho, \rho^2, \epsilon) \ ; \tag{76}$$

inserting (76) into $\mathcal{F}_K = 0$ we get the **bifurcation equation**, redefining $\mathcal{F}_K$ as

$$\mathcal{F}_K(v_\rho; k_\rho, \rho^2, \epsilon) := \mathcal{F}_K(v_\rho; k_\rho + h_\rho(v_\rho, k_\rho, \rho^2,\epsilon), \rho^2, \epsilon) \ , \tag{77}$$

where now

$$\mathcal{F}_K : \mathbb{R}^m\times\mathbb{R}\times\mathbb{R}\to\mathbb{R}^m \ ,$$

is defined once given the unperturbed reference solution v_ρ. An important characterization of $\mathcal{F}_K$ is that it vanishes with ϵ: this is true because equation $\mathcal{F}_K(v_\rho;k_\rho,\rho^2,0) = 0$ corresponds to the existence of the "coordinates" (k_ρ,h_ρ) describing the torus $\mathbb{T}^m$ around the chosen v_ρ. So that it is possible to introduce P_ρ as

$$\mathcal{F}_K(v_\rho;k_\rho,\rho^2,\epsilon) =: \epsilon P_\rho(v_\rho;k_\rho,\rho^2,\epsilon) \ , \tag{78}$$

and consequently (77) becomes

$$P_\rho(v_\rho;k_\rho,\rho^2,\epsilon) = 0 \ . \tag{79}$$

For a given v_ρ, we are interested in finding a small correction $k_\rho(\epsilon)\in\mathcal{U}(0)\subset\mathbb{R}^m$, continuous in ϵ for small enough $|\epsilon|\ll 1$, such that $P_\rho(v_\rho,k_\rho(\epsilon),\rho^2,\epsilon) = 0$. We now extend the notion of degeneracy already introduced in Definition 3.2

Definition 3.3. *We denote by* v_ρ^* *any solution of*

$$P_\rho(v_\rho;0,\rho^2,0) = 0 \ , \tag{80}$$

and by p *an integer such that*

$$dim\big(Ker\big(D_{k_\rho}P_\rho(v_\rho^*;0,\rho^2,0)\big)\big) = p+1 \ .$$

Then

1. v_ρ^* *is* non-degenerate *if* $p = 0$*;*
2. *a solution* $\phi_\rho = v_\rho^* + w_\rho(v_\rho^*, \epsilon)$ *of* (51) *is* non-degenerate *if* v_ρ^* *is non-degenerate;*
3. v_ρ^* *is* p-degenerate *if* $1 \leqslant p \leqslant m-1$.

Here again, thanks to the Lyapunov-Schmidt decomposition performed in the proof of Proposition 3.1, where higher harmonics included in w were implicitly defined as functions of the first harmonics in v, it is possible to show the following

Lemma 3.2. *The above equation* (80) *is equivalent (in the sense of coincidence of solutions) to the* persistence condition (10) *of the Effective Hamiltonian Method in the KG case, namely with* $M(\varphi)$ *given by* (12)*.*

Proof: In this case a direct method, as the one illustrated initially in the proof of Lemma 3.1, does not work and the variational Lyapunov-Schmidt approach is the route to understand the equivalence. First notice that, by the first Lyapunov-Schmidt decomposition, the system (10) is equivalent to applying the Effective Hamiltonian Method to the functional S_ρ defined in Proposition 3.2, namely to finding critical points of the average w.r.t. the periodic flow $e^{-i\tau}$ of the $\mathcal{O}(\epsilon)$ term of the S_ρ. Indeed, necessary conditions for the existence of periodic solutions of (26) must be recast into necessary conditions for the existence of corresponding periodic solutions of the equivalent equation (51). Then, the equivalence between this second system and (80) is a consequence of the second variational Lyapunov-Schmidt decomposition, using the same arguments already exploited in the proof of Lemma 3.1. □

The first Proposition of this Section shows that the non-degeneracy of v_ρ^* implies existence and uniqueness of a solution $\phi_\rho(v_\rho^*, \epsilon)$ of (51) for ϵ small enough.

Proposition 3.3. *Let* v_ρ^* *be a non-degenerate solution of the persistence condition* (80)*. Then, there exists* $\epsilon^*(v_\rho^*)$ *such that, for* $|\epsilon| < \epsilon^*$ *there exists* $k_\rho(\epsilon)$*, continuous in* ϵ*, which solves the bifurcation equation* (77)*.*

Proof: We consider the linearization around the origin of (80)

$$\epsilon \partial_\epsilon P_\rho(v_\rho^*; 0, \rho^2, 0) + D_{k_\rho} P_\rho(v_\rho^*; 0, \rho^2, 0)[k_\rho] = 0 \ . \tag{81}$$

Since by Proposition 3.2 the original equation (51) is equivariant under the gauge action, the same holds also for the bifurcation equation $P_\rho(v_\rho^*; k_\rho, \rho^2, \epsilon) = 0$. This involves the preservation of a symmetry under the Lyapunov-Schmidt reduction: indeed if the Kernel and Range projections commute with the symmetry, then also (77) is equivariant and it is enough to restrict to the orthogonal complement (see [20]). The non-degeneracy of v_ρ^* can be translated into the condition that the Kernel of the m-dimensional squared matrix $D_{k_\rho} P_\rho(v_\rho^*; 0, \rho^2, 0)$ is given only by the gauge direction, being invertible in the $m-1$-dimensional orthogonal complement, where the implicit function theorem applies. □

In the case of a degenerate v_ρ^*, next Proposition provides a direct criterion to show the nonexistence of the continuation, hence the nonexistence of a solution $\phi_\rho(v_\rho^*, \epsilon)$ of (51), continuous in ϵ, such that $\phi_\rho(v_\rho^*, 0) = v_\rho^*$.

Proposition 3.4. *Let* v_ρ^* *be a* p*-degenerate solution of the persistence condition* (80)*, such that the following conditions hold true*

$$rk\big(D_{k_\rho} P_\rho(v_\rho^*; 0, \rho^2, 0)\big) = m - p - 1 \ , \tag{h1}$$

$$\partial_\epsilon P_\rho(v_\rho^*; 0, \rho^2, 0) \not\equiv 0 \ . \tag{h2}$$

Then, a necessary condition for the continuation of v_ρ^* *for* $\epsilon \neq 0$ *is that*

$$\partial_\epsilon P_\rho(v_\rho^*; 0, \rho^2, 0) \in Range\big(D_{k_\rho} P_\rho(v_\rho^*; 0, \rho^2, 0)\big) \ . \tag{h3}$$

Proof:

The main idea is that, if $\partial_\epsilon P_\rho(v_\rho^*; 0, \rho^2, 0) \neq 0$ and at the same time the linearized equation (81) cannot be solved with respect to k_ρ, then in a small neighborhood of the origin the whole nonlinear equation does not admit solutions, namely $P_\rho(v_\rho^*; k_\rho, \rho^2, \epsilon) \neq 0$, because higher order corrections are negligible.

In more detail, we follow Lemma 4.4 and Remark 4.4 of [45]: one can implement a further Lyapunov-Schmidt decomposition, by splitting again the (m dimensional) space into the subspace $\mathrm{Ker}(D_{k_\rho} P_\rho(v_\rho^*; 0, \rho^2, 0))$, and the remaining $\mathrm{Range}(D_{k_\rho} P_\rho(v_\rho^*; 0, \rho^2, 0))$. This is possible thanks to condition (h1). In terms of variables, one simply introduces $k_{\mathscr{K}}$ and $k_{\mathscr{R}}$, the set of coordinates of $\mathrm{Ker}(D_{k_\rho} P_\rho(v_\rho^*; 0, \rho^2, 0))$ and $\mathrm{Range}(D_{k_\rho} P_\rho(v_\rho^*; 0, \rho^2, 0))$, respectively, such that $k_\rho = k_{\mathscr{K}} + k_{\mathscr{R}}$. After Taylor-expanding and projecting the equation $P_\rho(v_\rho^*; k_{\mathscr{K}}, k_{\mathscr{R}}, \rho^2, \epsilon) = 0$ onto the Range, one immediately realizes that $k_{\mathscr{R}} = \mathcal{O}(\epsilon)$. Thus, at leading order in the Kernel equation one has

$$\Pi_{\mathscr{K}}\big[\partial_\epsilon P_\rho(v_\rho^*; 0, \rho^2, 0)\big] = 0$$

which, if (h2) holds true, is equivalent to (h3). □

As already stressed concluding Section 3.1, in the totally degenerate case, when all v_ρ are solutions of (80), condition (h2) implies (h3), hence the last one is enough in order to show nonexistence of phase-shift solutions. This can be summarized in the following

Corollary 3.2. *Assume that* $P_\rho(v_\rho; 0, \rho^2, 0) \equiv 0$ *for all* v_ρ *and that for any* $v_\rho \neq v_{st}$ *the following condition is fulfilled*

$$\partial_\epsilon P_\rho(v_\rho; 0, \rho^2, 0) \not\equiv 0 \ , \tag{82}$$

Then the same as in Proposition 3.4 holds true.

Remark 3.3. *For an additional reading on the relationship between the linearized bifurcation equation* (81) *and the nonlinear equation* (80)*, we refer the interested reader to the more general statement of Proposition 2.10 of [41] (remark that, using the notation of the quoted paper, assumption* (h2) *would read* $g^{(2)}(\theta^*) \neq 0$*).*

Step C: within the (generalized) dNLS family

A direct application of Propositions 3.3 and 3.4 requires an explicit knowledge of the remainder $\mathscr{R}_\rho$ in (51), which is implicitly defined in its part $\mathsf{w}(\mathsf{v}, \epsilon)$ in (67). In this Section we show the validity of these Propositions on the basis of the analysis of its leading part (32). As a result of this analysis, Theorems 3.1 and 3.2 will be proved.

The main equation, which provides all the information about our problem of continuation, is given by (79). The next Proposition allows us to treat the bifurcation equation (79) as a smooth perturbation of order $\mathcal{O}(\rho^2)$ of equation (41):

Proposition 3.5. *The function $P_\rho(v_\rho; k_\rho, \rho^2, \epsilon)$ is smooth in ρ^2 and fulfills*

$$P_\rho(v_\rho; k_\rho, \rho^2, \epsilon)\Big|_{\rho=0} = P(v; k, \epsilon) \ . \tag{83}$$

Proof: Equation (74) is plainly smooth in all its variables due to Proposition 3.1; when evaluated at $\rho = 0$, it becomes exactly equation (36), and reduces to the dNLS model analyzed in Section 3.1

$$\mathcal{F}(v_\rho; w, \rho^2, \epsilon)|_{\rho=0} \equiv F(v; w, \epsilon) \ . \tag{84}$$

Thus, equation (74) may be expanded as

$$\mathcal{F}(v_\rho; w, \rho^2, \epsilon) := F(v; w, \epsilon) + \mathcal{O}(\rho^2) \ . \tag{85}$$

Observe also that the projections on $\mathrm{Ker}(\Lambda_\rho)$ and $\mathrm{Range}(\Lambda_\rho)$ are smooth in ρ^2, which implies the same regularity for the function $\mathcal{F}_H$ and for the implicitly defined solutions $h_\rho(v_\rho; k_\rho, \rho^2, \epsilon)$ of $\mathcal{F}_H = 0$. This provides the smoothness of $\mathcal{F}_K(v_\rho; k_\rho, \rho^2, \epsilon)$ and eventually of P_ρ

$$\epsilon P_\rho = \mathcal{F}_K \ .$$

As for $\mathcal{F}$, also for P_ρ it holds

$$P_\rho(v_\rho; k, \rho^2, \epsilon)\Big|_{\rho=0} = P(v; k, \epsilon) \ ,$$

which concludes the proof. □

3.3.1. Proof of Theorem 3.1

The proof of Theorem 3.1 mainly follows from the fact that non-degenerate solutions v^* can be continued to a family, in the parameter ρ, of non-degenerate solutions v^*_ρ:

Lemma 3.3. *Let v^* be a non-degenerate solution of (42). Then, there exists ρ^* such that, for $|\rho| < \rho^*$ there exists a unique (modulo gauge transformation) and non-degenerate v^*_ρ, solution of (80) which is smooth with respect to ρ^2 and fulfills*

$$v^*_\rho = v^* + \mathcal{O}(\rho^2) \ .$$

Proof:

The proof can be obtained applying the implicit function theorem to (80), since from the previous Proposition one has

$$P_\rho(v_\rho; 0, \rho^2, 0)\Big|_{\rho=0} = P(v; 0, 0) \ .$$

The nondegeneracy of the approximated solution v^* provides the existence (modulo Gauge transformation) of v^*_ρ. Its nondegeneracy is given by the smoothness of the Lyapunov-Schmidt decomposition with respect to the small parameter ρ, which provides the invertibility of the differential $D_{k_\rho} P_\rho(v^*_\rho; 0, \rho^2, 0)$ on the subspace orthogonal to the Gauge, for ρ small enough. The ρ^2-expansion of v^*_ρ is a consequence of its smoothness with respect to ρ^2. □

The above Lemma allows to apply Proposition 3.3 of Step B, in the limit of ρ small enough, thus ensuring the existence of a solution $\phi_\rho(\epsilon)$ bifurcating from $\phi^*(\rho)$, with $\rho < \rho^*$. In order to conclude the proof of Theorem 3.1, we still have to show that (44) holds true. Let now $w^*_\rho(v^*_\rho; \epsilon)$ be the solution of

$$\mathcal{F}(v^*_\rho; w, \rho, \epsilon) = 0 \ ,$$

and, in a similar way, let $w^*(v^*; \epsilon)$ be the solution of

$$F(v^*; w, \epsilon) = 0 \ .$$

Lemma 3.4. *There exists ρ^* and ϵ^* such that, for $|\rho| < \rho^*$ and $\epsilon < \rho^2 \epsilon^*$ one has*

$$w^*_\rho(v^*_\rho; \epsilon) = w^*(v^*; \epsilon) + \mathcal{O}(\rho^2) \ . \tag{86}$$

Proof: From the smoothness of the solution h_ρ of the Range equation $\mathcal{F}_H = 0$ one gets

$$h_\rho(v^*_\rho; k_\rho, \rho^2, \epsilon) = h(v^*; k, \epsilon) + \mathcal{O}(\rho^2) \ . \tag{87}$$

In a similar way, the solution $k_\rho(v^*_\rho; \epsilon)$ of $\mathcal{F}_K = 0$ given by the implicit function theorem also satisfies the leading order approximation

$$k_\rho(v^*_\rho; \epsilon) = k(v^*; \epsilon) + \mathcal{O}(\rho^2) \ , \tag{88}$$

hence the estimate easily follows recalling that

$$\begin{aligned} w^*_\rho(v^*_\rho; \epsilon) &= k_\rho(v^*_\rho; \epsilon) + h_\rho(v^*_\rho; k_\rho, \rho^2, \epsilon) = \\ &= k(v^*; \epsilon) + h(v^*; k, \epsilon) + \mathcal{O}(\rho^2) = \\ &= w^*(v^*; \epsilon) + \mathcal{O}(\rho^2) \ . \end{aligned}$$

□

Going back to (55), let $\mathsf{v}^*(\rho, \epsilon, \tau)$ and $\mathsf{v}^*(0, \epsilon, \tau)$ be the scaled real solutions (belonging to the Kernel V_2) built respectively with $\phi^*_\rho(\epsilon) = v^*_\rho + w^*_\rho(v^*_\rho; \epsilon)$ and $\phi^*(\epsilon) = v^* + w^*(v^*; \epsilon)$, where

$$\phi^*_\rho(\epsilon) = \rho \phi^*(\epsilon) + \mathcal{O}(\rho^3) \ , \tag{89}$$

and let

$$u^*(\rho, \epsilon, \tau) = \mathsf{v}^*(\rho, \epsilon, \tau) + \mathsf{w}(\mathsf{v}^*(\rho, \epsilon, \tau), \epsilon) \ , \tag{90}$$

be the reconstructed real solution of the original perturbed problem (30): from the previous leading order approximation (89) and from $\mathsf{w} = \mathcal{O}(\|\mathsf{v}\|^3) = \mathcal{O}(\rho^3)$ one gets (44).

3.3.2. Proof of Theorem 3.2

The proof of Theorem 3.2 is based on a necessary condition for the solvability of the bifurcation equation which is shown to be violated at v^*_ρ, as stated in Proposition 3.4. Given the difficulty to verify the assumptions in Proposition 3.4 directly on the equation (79), the strategy is to derive their validity from the hypothesis (H1)-(H3) of Theorem 3.2. However, differently from the non-degenerate case, where solutions v^* and v^*_ρ can be easily connected in the limit of small ρ, degenerate solutions of (79) might differ from those of (41), even for an arbitrarily small perturbation. Indeed, a degenerate v^* can decrease its class of degeneracy due to an arbitrarily small perturbation, if it removes at least one of the Kernel direction; and moreover, nondegeneracy in the remaining directions cannot be lost. From here, stems the choice to restrict the treatment to those cases fulfilling the main Assumption (H0). This additional requirement states that degenerate solutions v^* and v^*_ρ differ only for the amplitude, and not for the phases $\{\theta_l\}_{l \in S}$.

Proposition 3.6. *Given (H0), assume that any p-degenerate $v^* \neq v^*_{st}$ is such that*

$$\begin{aligned} &\partial_\epsilon P(v^*; 0, 0) \not\equiv 0 \ , \\ &rk(D_k P(v^*; 0, 0)) = m - p - 1 \ , \\ &\partial_\epsilon P(v^*; 0, 0) \notin Range(D_k P(v^*; 0, 0)) \ , \end{aligned} \tag{91}$$

then for any degenerate $v^*_\rho \neq v^*_{\rho,st}$ there exists $\rho^*(v^*)$ such that, for $|\rho| < \rho^*$ one has

$$\partial_\epsilon P_\rho(v^*_\rho, 0, \rho^2, 0) \not\equiv 0 \ ,$$
$$rk\big(D_{k_\rho} P_\rho(v^*; 0, \rho^2, 0)\big) = m - p - 1 \ ,$$
$$\partial_\epsilon P_\rho(v^*_\rho, 0, \rho^2, 0) \notin Range\big(D_{k_\rho} P_\rho(v^*_\rho, 0, \rho^2, 0)\big) \ .$$

Proof:

Because of Assumption (H0), given any degenerate v^*_ρ, by continuity in the limit of $\rho \to 0$ it converges to the corresponding degenerate v^*, having the same phases θ_l and amplitude equal to 1. Whatever is the degree of degeneracy of the limit solution v^*, the same type of degeneracy holds also for v^*_ρ, at least for ρ small enough. Hence $D_k P(v^*; 0, 0)$ and $D_{k_\rho} P_\rho(v^*; 0, \rho^2, 0)$ have the same spectral properties and the hypothesis on the $\mathrm{rk}\big(D_{k_\rho} P_\rho(v^*; 0, \rho^2, 0)\big)$ is true. The other two properties concerning $\partial_\epsilon P_\rho(v^*_\rho, 0, \rho^2, 0)$ are simply a consequence of the smoothness with respect to ρ^2. □

Now, in order to conclude the proof of the Theorem 3.2, let us assume that there exists a degenerate $v^*_\rho \neq v^*_{\rho,\mathrm{st}}$, and then a corresponding $\bar{u} \neq \bar{u}_{\mathrm{st}}$, which can be continued: then, as a necessary condition for the continuation, assumption (h3) of Proposition 3.4 has to hold, and using Proposition 3.6 one realizes that assumption (H3) of Proposition 3.4 is violated.

Remark 3.4. *It is natural to ask how to reconcile the nonexistence of the continuation for phase-shift solutions v^*_ρ with the existence of the continuation for standard solutions v^*_{st}, given that they may belong to the same family. The point is that, as it could be shown combining the above Proposition 3.6 with Proposition 3.4, the nonexistence result is "local" in amplitude up to a certain threshold $\rho^*(v^*)$ which depends on v^*. As it will be more clear in the next applications, where $\partial_\epsilon P(v^*; 0, 0)$ is explicitly computed, the threshold $\rho^*(v^*)$ has to vanish as $v^* \to v^*_{st}$; indeed we have already recalled that standard solutions always exist (both in the KG and in the corresponding dNLS model) and hence the proposed criterion has to fail at $v^* = v^*_{st}$.*

4. Applications

In Section 2 we have shown three different examples where the Effective Hamiltonian Method could not be applied, due to degeneracies in the persistence conditions; as a consequence, despite the differences of the mechanism leading to the degeneracy, in all the cases it was not possible to establish the existence of phase-shift Multibreathers.

In the present Section we show how to apply Theorem 3.2, and Corollary 3.1, in order to prove that in all the above mentioned examples only standard Multibreathers can be continued at $\epsilon \neq 0$, in the limit of small enough energy. This is performed by showing the validity of the assumptions (H1)-(H3) in the dNLS equation (32), since the validity of (H0) has been already discussed in Section 2 itself. In particular, with the last application of this Section we are going to prove Theorem 1, which is stated in the Introduction, about the four-site vortex-like solutions in the zigzag KG model.

Let us rewrite explicitly the specific dNLS equation (32) we consider here, i.e.,

$$\omega_0 \phi_j = -\frac{\epsilon}{2}\Big[(\Delta_1 + \kappa_2 \Delta_2)\phi\Big]_j + \frac{3}{4}\phi_j |\phi_j|^2 \ , \tag{92}$$

where κ_2 can be either 0 or 1, depending on the models considered in the application, and the unperturbed solutions v read

$$v_l = \begin{cases} e^{-i\theta_l} \ , & l \in S \ , \\ 0 \ , & l \notin S \ , \end{cases} \tag{93}$$

where $S = \{j_1, \ldots, j_m\}$ will depend on the example.

The statements of Theorem 3.1 and Corollary 3.1 require the computation of $\partial_\epsilon P(v^*; 0, 0)$, which explicitly reads

$$\partial_\epsilon P(v^*; 0, 0) = -\Pi_K L \Lambda^{-1} \Pi_H L v^* \ , \tag{94}$$

and possibly also its projection on the Kernel of $D_k P(v^*; 0, 0)$; indeed, since $D_k P(v^*; 0, 0)$ is self-adjoint, the condition (H3) is equivalent to

$$\partial_\epsilon P(v^*; 0, 0) \not\perp \mathrm{Ker}(D_k P(v^*; 0, 0)) \ .$$

Once introduced phase-shift variables φ_l as in (7) in the definition of v given by (33), equation (80) turns out to be independent of the "last angle" θ_{j_1}: hence solutions v^* are always given by loops on the torus $\mathbb{T}^m$ and are uniquely represented by a value $\boldsymbol{\varphi}$ on the torus $\mathbb{T}^{m-1} := \mathbb{T}^m / \mathbb{T}$.

In practice, projections over vectors belonging to K are performed using the complex inner scalar product $a \cdot b = \sum_j \Re(a_j \bar{b}_j)$, where a basis $\{e_l\}_{l=1,\ldots,m}$ for K is given by

$$\{e_l\}_{l=1} = -\partial_{\theta_{j_1}} v \ (\theta_{j_1}, \boldsymbol{\varphi}) \ , \qquad \{e_l\}_{l \geqslant 2} = \partial_{\varphi_l} v^*(\theta_{j_1}, \boldsymbol{\varphi}) \ .$$

4.1 Simpler examples: degeneracy from holes

The two cases included in this Subsection represent examples of complete degeneracy, where $P(v; 0, 0) = 0$ for any $v \in \mathbb{T}^m$. In both the examples, the complete degeneracy comes out from the interplay between the presence of a hole in the configuration S and the minimal dimension of the torus $m = 2$. In these cases, application of Theorem 3.2 reduces to Corollary 3.1: thus it is enough to check that

$$\partial_\epsilon P(v^*; 0, 0) \neq 0 \ , \qquad \forall v^* \neq v^*_{\mathrm{st}} \ .$$

4.1.1. $S = \{-1, 1\}$ in the standard KG model

In this case

$$v^*(\theta_1, \varphi) = \Big[\ldots, 0, e^{-i\theta_1}, 0, e^{-i(\theta_1 + \varphi)}, 0, \ldots\Big] \ .$$

The Kernel's basis computed on a generic element of the family, setting $\theta_1 = 0$, reads

$$\boldsymbol{e_1} = i\Big[\ldots, 0, 1, 0, e^{-i\varphi}, 0, \ldots\Big] \ ,$$
$$\boldsymbol{e_2} = i\Big[\ldots, 0, 0, 0, e^{-i\varphi}, 0, \ldots\Big] \ .$$

A straightforward computation gives the restriction of $L\Lambda^{-1}\Pi_H L v^*$ to the components corresponding to the set of sites S, which are the only ones relevant for the projection on K

$$-\big(L\Lambda^{-1}\Pi_H L v^*\big)\Big|_S = \frac{1}{2\omega_0}\Big[1, e^{-i\varphi}\Big] \ ;$$

in the above calculation, the projection Π_H on the range has been simplified

$$L\Lambda^{-1}\Pi_H L v^* = L\Lambda^{-1} L v^* \ ,$$

due to the fact that $\Pi_K L v^* = 0$ by definition. This allows to get

$$-L\Lambda^{-1}\Pi_H L v^* \cdot \boldsymbol{e_1} = 0 \ , \qquad -L\Lambda^{-1}\Pi_H L v^* \cdot \boldsymbol{e_2} = -\frac{\sin(\varphi)}{\omega_0} \ ,$$

hence $\partial_\epsilon P(v^*; 0, 0) \neq 0$ for all $\varphi \notin \{0, \pi\}$.

4.1.2. $S = \{1, 4\}$ in the zigzag KG model

In this case

$$v^*(\theta_1, \varphi) = \Big[\dots, 0, e^{-i\theta_1}, 0, 0, e^{-i(\theta_1+\varphi)}, 0, \dots\Big] .$$

The Kernel's basis computed on a generic element of the family, setting $\theta_1 = 0$, reads

$$\boldsymbol{e_1} = i\Big[\dots, 0, 1, 0, 0, e^{-i\varphi}, 0, \dots\Big] ,$$
$$\boldsymbol{e_2} = i\Big[\dots, 0, 0, 0, 0, e^{-i\varphi}, 0, \dots\Big] .$$

A straightforward computation gives the restriction

$$-\big(L\Lambda^{-1}\Pi_H L v^*\big)\Big|_S = -\frac{1}{4\omega_0}\Big[e^{-i\varphi} - 5, 1 - 5e^{-i\varphi}\Big] ,$$

which allows to get

$$-L\Lambda^{-1}\Pi_H L v^* \cdot \boldsymbol{e_1} = 0 , \qquad -L\Lambda^{-1}\Pi_H L v^* \cdot \boldsymbol{e_2} = -\frac{\sin(\varphi)}{4\omega_0} ,$$

hence $\partial_\epsilon P(v^*; 0, 0) \neq 0$ for all $\varphi \notin \{0, \pi\}$.

4.2. Subtler example: degeneracy due to symmetry; $S = \{1, 2, 3, 4\}$ in the zigzag model

In this case, we consider the zigzag model given by $\kappa_2 = 1$ and the vortex-like configurations described by the set $S = \{1, 2, 3, 4\}$. As already commented in Section 2, this represents a prototype example of a more complex type of degeneracy, which is indeed related to "internal" symmetries of the configurations.

Differently from the previous easier examples, where the degeneracy was total and the application of Corollary 3.1 was enough, now we have to check the projection of $\partial_\epsilon P(v^*, 0, 0)$ given by (94) onto the Kernel of the linear operator $D_k P(v^*, 0, 0)$, with v^* belonging to the families F_1 and F_2. We deal explicitly with one family only, namely $F_1 : \boldsymbol{\varphi} = (\varphi, \pi, -\varphi)$; by setting $\theta_1 = 0$, we have $\boldsymbol{\theta} = (0, \pi, -\varphi, \pi)$, which gives the following representation of v^* in complex variables

$$v^*(\varphi) = \Big[\dots, 0, 1, e^{-i\varphi}, -e^{-i\varphi}, -1, 0, \dots\Big] .$$

The Kernel's basis computed on a generic element of the family $F_1(\boldsymbol{\varphi})$ reads[3]

$$\boldsymbol{e_1} = i\Big[\dots, 0\Big|1, e^{-i\varphi}, -e^{-i\varphi}, -1\Big|0, \dots\Big] ,$$
$$\boldsymbol{e_2} = i\Big[\dots, 0\Big|0, e^{-i\varphi}, -e^{-i\varphi}, -1\Big|0, \dots\Big] ,$$
$$\boldsymbol{e_3} = i\Big[\dots, 0\Big|0, 0, -e^{-i\varphi}, -1\Big|0, \dots\Big] ,$$
$$\boldsymbol{e_4} = i\Big[\dots, 0\Big|0, 0, 0, -1\Big|\dots\Big] .$$

An easy computation gives Lv^*, precisely

$$\Big[\dots, 0, 1, 1 + e^{-i\varphi}\Big| - 4, 5e^{-i\varphi}, 5e^{-i\varphi}, 4\Big| - (1 + e^{-i\varphi}), -1, 0, \dots\Big] ;$$

since

$$\Lambda h = \begin{cases} -2\omega_0 h , & j \in S \\ \omega_0 h , & j \notin S \end{cases} ,$$

then $-\Lambda^{-1}\Pi_H L v^*$ takes the form

$$\frac{1}{\omega_0}\Big[\dots, 0, -1, -(1 + e^{-i\varphi})\Big| - 2, \frac{5}{2}e^{-i\varphi}, \frac{5}{2}e^{-i\varphi}, 2\Big|(1 + e^{-i\varphi}), 1, 0, \dots\Big] .$$

Given that our last operation is a projection onto the Kernel, we limit the next computation on the restriction $-\big(L\Lambda^{-1}\Pi_H L v^*\big)\Big|_S$, which reads

$$\frac{1}{\omega_0}\Big[6 - e^{-i\varphi}, \frac{23}{2} \dots - 1, -\frac{23}{2}e^{-i\varphi} + 1, -6 + e^{-i\varphi}\Big] .$$

A direct computation shows that

$$-L\Lambda^{-1}\Pi_H L v^* \cdot \boldsymbol{e_{1,3}} = 0 , \qquad -L\Lambda^{-1}\Pi_H L v^* \cdot \boldsymbol{e_{2,4}} = \pm\frac{\sin(\varphi)}{\omega_0} .$$

Upon verifying that the four-dimensional matrix representing the linear operator $D_k P(v^*, 0, 0)[k]$ has rank 2, we know for free the Kernel generators, since the gauge direction and the direction tangent to the family for sure belong to it; these are respectively

$$\partial_\varphi v^*(\varphi) = \boldsymbol{e_2} - \boldsymbol{e_4} , \qquad \partial_{\theta_1} e^{i\theta_1} v^*(\varphi) = \boldsymbol{e_1} .$$

The previous scalar projections of $-L\Lambda^{-1}\Pi_H L v^*$ on the basis $\{\iota\}_{l=1,\dots,4}$ show that

$$\dots \cdot \partial_\epsilon P(v^*, 0, 0) = 0 , \qquad \partial_\varphi v^*(\varphi) \cdot \partial_\epsilon P(v^*, 0, 0) = \frac{2}{\omega_0}\sin(\varphi) ,$$

which is different from zero, apart from the cases $\varphi \in \{0, \pi\}$. Thus, we can conclude that the projection of $\partial_\epsilon P(v^*(\varphi); 0, 0)$ onto the Kernel of $D_k P(v^*; 0, 0)$ is different from zero on any phase-shift discrete soliton considered in the family F_1. Since the same holds true also for the second family F_2, this represents a sufficient condition for nonexistence of the continuation of any phase-shift Multibreather corresponding to $S = \{1, 2, 3, 4\}$.

4.3. A note on an even more degenerate model

As already observed in the final part of the Introduction, the technique developed in this Section is not sufficient to deal with the more degenerate model considered in Section 2.4.2, i.e., $\mathscr{H}_{101}$ in (17). Actually this kind of degeneracy in a dNLS model was already examined systematically in [45], where we were able to prove the nonexistence of any four-sites phase-shift discrete soliton for ϵ small enough. The crucial point is that the higher non-degeneracy required in that paper the analysis of higher order expansions of the Bifurcation Equation: this is exactly the reason that prevents the application of the techniques used here. Indeed the small perturbation due to the energy, which "measures" the distance between the KG model (17) and its dNLS-type normal form (23), could be enough to introduce small linear terms in the bifurcation equation allowing for non-trivial solutions, which otherwise would not exist. This, however, depends on the magnitude of the linear term in ϵ introduced by the perturbation. Since the obstruction to nonexistence comes out from the ϵ^2 term in the Kernel equation, the corrections of order ρ^2 would be relevant in the regime $\epsilon \lesssim \rho^2$ here considered.

[3] We will use the notation $[\dots|\cdot,\cdot,\cdot,\cdot|\dots]$ to denote values along the chain: in particular, the two vertical bars enclose the sites belonging to S, when indexes j_i are consecutive.

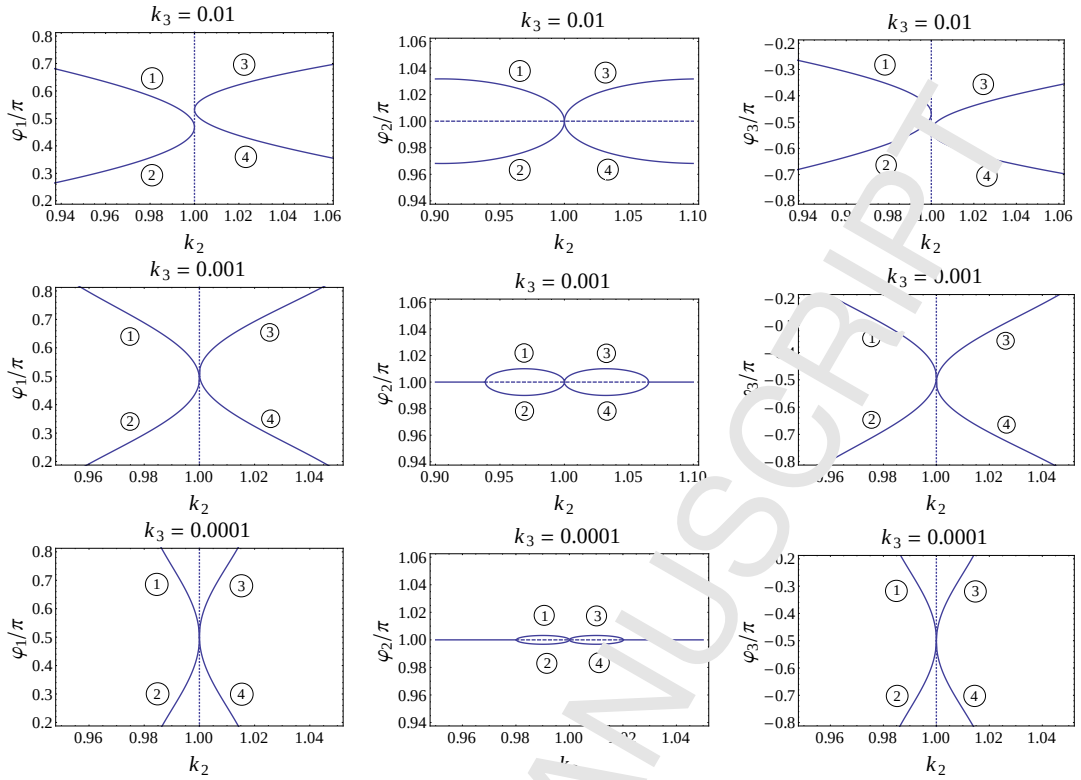

Figure 6: The bifurcation diagrams of the persistence condition (95), in the k-parameter region corresponding to the zigzag ($\mathscr{H}_{110}$) model and in the $\boldsymbol{\varphi}$-region of $\Phi^{(\mathrm{sv})}$. The rows of the figure correspond to the three distinct values of k_3, i.e. $k_3 = 0.01, 0.001, 0.0001$, where the diagrams for an interval of k_2 in the specific region are shown. The three columns correspond to the values of the three φ_i which constitute the various solution-families. The distinct branches are characterized by encircled numbers, while their exact combination for each family can be found in Table 2. The family $F_1 : \boldsymbol{\varphi} = (\varphi, \pi, -\varphi)$ is degenerate (possesses one 0 eigenvalue) and it is represented by a dotted line at $k_2 = 1$. Negative values of k_3 are not considered since for $k_3 < 0$, there exist no relevant phase-shift solution families.

5. Numerical study

In this section we will perform a numerical study of the persistence conditions which correspond to the system (2) in an attempt to showcase the degeneracy of the configurations of the $\mathscr{H}_{110}$ (zigzag) and the $\mathscr{H}_{101}$ (inspired by the 2d square lattice) models which have been already discussed in section 2. These conditions are given by

$$\mathcal{P}(\boldsymbol{\varphi}) \equiv \begin{cases} M(\varphi_1) + k_2 M(\varphi_1 + \varphi_2) + k_3 M(\varphi_1 + \varphi_2 + \varphi_3) = 0 \\ M(\varphi_2) + k_2 M(\varphi_1 + \varphi_2) + k_2 M(\varphi_2 + \varphi_3) \\ \qquad\qquad + k_3 M(\varphi_1 + \varphi_2 + \varphi_3) = 0 \\ M(\varphi_3) + k_2 M(\varphi_2 + \varphi_3) + k_3 M(\varphi_1 + \varphi_2 + \varphi_3) = 0 \end{cases} \tag{95}$$

with M as in (12). Note that since we consider low amplitude solutions, the results for the Klein-Gordon and dNLS variants of the system are equivalent both qualitatively as well as quantitatively, since the differences in the solutions are negligible. Thus, we could have used (20) instead.

We will focus mainly on the parametric regions corresponding to the above mentioned systems, namely $k_2 = 1, k_3 = 0$ and $k_2 = 0, k_3 = 1$ for the $\mathscr{H}_{110}$ and $\mathscr{H}_{101}$ systems respectively.

The illustration of the degeneracy will occur by showing the convergence of various solution families as the k_2, k_3- parameters tend to the ones corresponding to the cases under examination. Hopefully, by this procedure we will also be able to underline the difference in the degeneracy "magnitude" between the two systems since in the zigzag model only two solution families converge, while in the $\mathscr{H}_{101}$ model there exist three converging families.

5.1. Study near $k_2 = 1, k_3 = 0$

First we examine the parametric region corresponding to the zigzag system (namely near $k_2 = 1, k_3 = 0$). In this study, a crucial role is played by the two families F_1 and F_2 of asymmetric vortices solutions of (11) which are given by (14).

The proper representation of the solutions of (95) would require a three-dimensional plot for every phase-difference φ_i as a function of both k_2 and k_3. Since this surface is difficult to be properly illustrated, we prefer to present some sections, first for fixed k_3, varying k_2, and then by reversing the roles between k_2 and k_3.

The results of the study for this parameter-region are found in Figs. 6 and 7. Let's examine first Figure 6. The first thing one can observe is the existence of the $F_1 : \boldsymbol{\varphi} = (\varphi, \pi, -\varphi)$ family of solutions which is depicted as a vertical line at $k_2 = 1$, in the diagrams for the φ_1 and φ_3 slow variables. Note that, F_1 satisfies the persistence conditions (95) for every value of k_3 and $k_2 = 1$ as it is easy to verify by substituting the values of $\boldsymbol{\varphi}$ which correspond to F_1 into (95). On the other hand, for $k_3 > 0$ we observe that there exist two phase-shift families, which bifurcated from the symmetric vortex configuration $\boldsymbol{\varphi} = \Phi^{(\mathrm{sv})} = (\pi/2, \pi, -\pi/2)$. Each depicted family is determined by

its values of φ_i's and it is detailed in Table 2 (e.g., family 1 consists of the $\varphi_1 = ①$, $\varphi_2 = ②$, $\varphi_3 = ②$ in Figure 6, etc.).

♯ of Family	Branch description		
	φ_1	φ_2	φ_3
1	①	②	②
2	②	①	①
3	③	③	④
4	④	④	③

Table 2: The solution families depicted in Figure 6.

We can see that the bifurcation points of the phase-shift families under consideration approach $\Phi^{(\mathrm{sv})}$ and the families themselves tend to coincide with the F_2 family (14) as $k_3 \to 0$. For $k_3 = 0$ the families coincide with F_2 which visually coincides also with F_1. The F_1 and F_2 families really cross each other at $\Phi^{(\mathrm{sv})}$. The not so illustrative bifurcation diagrams for $k_3 = 0$ would be just a vertical line at $k_2 = 1$ in the φ_1 and φ_3 diagrams and a horizontal line at $\phi_2 = \pi$. Note that, there are no bifurcation diagrams for $k_3 < 0$ since for these values there exist no relevant solution families.

The degeneracy of the system is revealed by the fact that all the phase-shift families merge to the F_1 and F_2 ones and the fact the the matrix (16) has the specific form at $\Phi^{(\mathrm{sv})}$ is due to the family crossing at this point revealing the two kernel directions of the persistence condition.

The same behavior is also suggested in Figure 7, where two monoparametric variations over k_3 are now given for a set of values of k_2 progressively approaching $k_2 = 1$. More specifically, k_2 has been chosen close to, but less than, 1 and k_3 left free to vary around 0. The two families which are depicted in Figure 7 are the ones shown in Table 3. We can observe in a more clear way the difference between the $k_3 \leqslant 0$ case and the $k_3 > 0$ case, in terms of phase-shift solutions. When $k_3 > 0$ there are branches connecting (apparently) to 0 and π: although the situation very close to $k_3 = 0$ is not perfectly shown, it is anyway evident that the branches in the upper and lower parts of the frames get closer and closer as $k_2 \to 1$, like converging to a curve which emerges from $\Phi^{(\mathrm{sv})}$. At exactly $k_2 = 1$, one should observe a full band for the phase differences $\varphi_{1,3}$. In this representation the F_1 family is not shown since it exists only for $k_2 = 1$. The picture is completely symmetrical to the one of Figure 7 in the $k_2 >$ case.

♯ of Family	Branch description		
	φ_1	φ_2	φ_3
1	①	②	①
2	②	①	②

Table 3: The solution families depicted in Figure 7.

The overall picture emerging from the above numerical exploration is the following. Whenever $k_2 \neq 1$, solutions appear to be isolated, thus non-degenerate and suitable to be continued. Nonetheless, as $k_2 \to 1$, their non-degeneracy gets weaker and weaker, so that the domain of continuation in the coupling parameter ϵ is expected to vanish, according to the standard estimate given by the implicit function theorem. The degenerate scenario which appears at $k_2 = 1$, due to the existence of a one-parameter family of solutions F_1 for generic values of k_3, becomes richer at $k_3 = 0$, since a second family F_2 arises which intersects the already existing F_1 at $\Phi^{(\mathrm{sv})}$. The possibility to continue such degenerate solutions requires the more accurate mathematical analysis, that we developed in Section 3 and applied in this model in Section 4.

5.2. Study near $k_2 = 0$, $k_3 = 1$

The next numerical study we are going to perform is the one of the solutions of (95), close to the $k_2 = 0, k_3 = 1$ parametric area which corresponds to the $\mathscr{H}_{101}$ model. The results of this study appear in Figs. 8, 9 and 10.

First, in Figure 8 we present the bifurcation diagrams of (95) for some values of $k_3 < 1$ (in particular for $k_3 = 0.9, 0.99$ and 0.999) and an interval of k_2 around $k_2 = 0$. In the top row the values of the angles φ_1 and φ_3 are shown while the bottom row depicts the values of φ_2. Although, the φ_1 and φ_3 angles are depicted in the same diagram, this does not mean that $\varphi_1 = \varphi_3$ for every value of k_2. The four families which are shown in Figure 8 are labeled with encircled numbers and are summarized in Table 4 below (e.g., family 1 is defined as $\varphi_1 = ①$ of the upper row of the figure, $\varphi_2 = ①$ of the lower row and $\varphi_3 = ②$ of the upper row panels). We see in these diagrams how these families converge to the $k_2 = 0$ asymptote. In particular, families 1 and 4 converge to F_3, while families 2 and 3 converge to F_1 (19). The different line symbols denote different linear stability of the families. In particular a solid line corresponds to a family with one unstable eigenvalue while the dashed line corresponds to two unstable eigenvalues. As the families converge one of their stability eigenvalue converges to zero and it changes sign when k_2 crosses zero. Since the stability discussion lies outside the scope of the present manuscript we will not refer further to the relevant details. We only mention this for the bifurcation theory inclined numerical reader who may appreciate some of the associated bifurcations, such as the pitchforks in Figure 9.

♯ of Family	Branch description		
	φ_1	φ_2	φ_3
1	①	①	②
2	②	①	①
3	③	②	④
4	④	②	③

Table 4: The solution families depicted in Figure 8

Next, we consider the bifurcation-diagrams for $k_3 > 1$ (In particular $k_3 = 1.1$, 1.01 and 1.001) which are depicted in Figure 9. We can clearly observe that families 1 and 4 of Table 5 below converge into F_3 as $k_3 \to 1$ while families 2 and 3 converge to F_1. The main difference of this diagrams, with respect to the ones of the $k_3 < 1$ case, is that in this case there exist also the two new phase-shift solution families 5 and 6, where the families 1-4 bifurcate from through pitchfork bifurcations. These families also have the characteristic that they are the only ones that exist for $k_2 = 0$ and for all $k_3 > 0$.

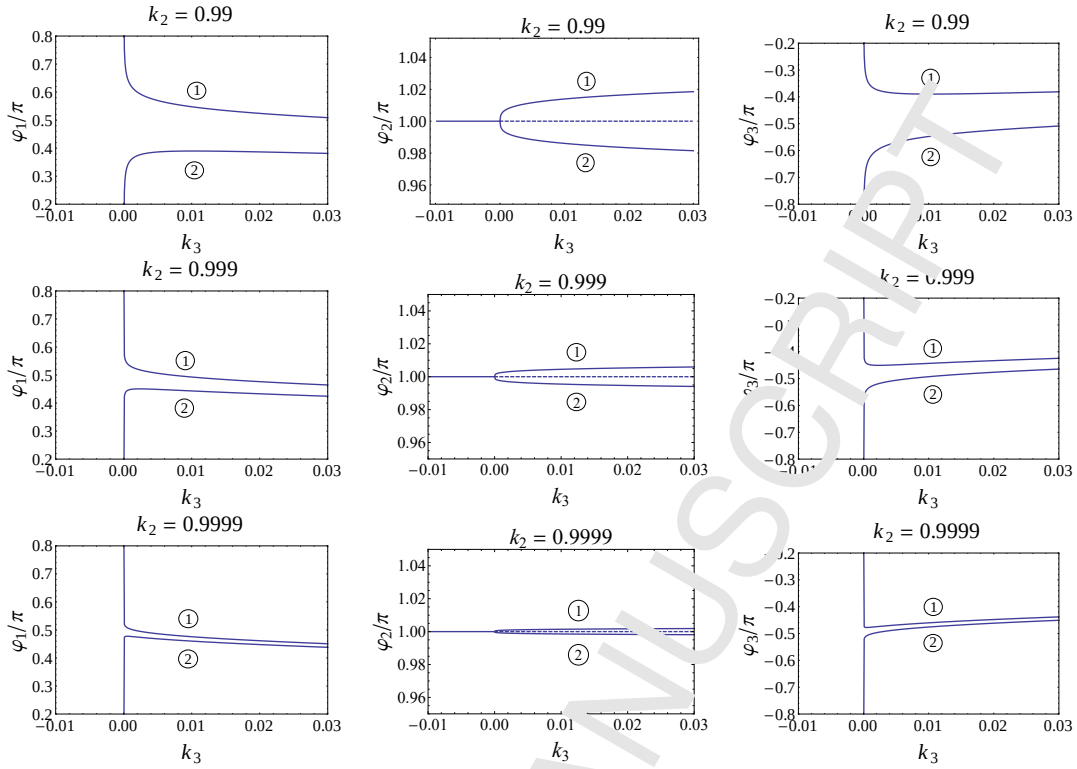

Figure 7: The bifurcation diagrams of the persistence condition (95), in the k-parameter region corresponding to the zigzag ($\mathscr{H}_{110}$) model and in the $\boldsymbol{\varphi}$-region of $\Phi^{(\mathrm{sv})}$. The rows of the figure correspond to three distinct values of k_2, i.e. $k_2 = 0.99, 0.999, 0.9999$, where the diagrams for an interval of k_3 in the specific region are shown. The three columns correspond to the values of the three φ_i which constitute the various solution-families. The distinct branches are characterized by encircled numbers, while their exact combination for each family can be found in Table 3. Note that for $k_3 < 0$ there exist no relevant phase-vortex solution families.

♯ of Family	Branch description		
	φ_1	φ_2	φ_3
1	①	①	②
2	②	①	①
3	③	②	④
4	④	②	③
5	⑤	③	⑤
6	⑥	④	⑥

Table 5: The solution families depicted in Figure 9.

For $k_3 = 1$, the Jacobian is highly degenerate and hence we show no frame for this value of k_3. Nevertheless, it is straightforward to see that the three families F_1, F_2 and F_3 coincide at this value of k_3.

In order to demonstrate this fact better, as well as to better show the role of the families 5 and 6 of the $k_3 > 1$ case, we consider the role of k_2 and k_3 variations between Figs. 9 and 10. In the latter case we consider specific values of k_2 close to $k_2 = 0$ (i.e., $k_2 = -0.001, -0.0001, 0.0001, 0.001$) and an interval of values around $k_3 = 1$ and examine the bifurcation diagrams of (95). First of all we can see the family $F_2 : \boldsymbol{\varphi} = (\varphi, \pi - \varphi, \varphi)$ which exists for $k_3 = 1$ and every value of k_2. Since this family is degenerate it is depicted as a dotted line. The rest of the families depicted there are shown in Table 6 below.

We can see that families 1 and 4 tend to F_1 while families 2 and 3 tend to F_3 as $k_2 \to 0$. Geometrically this is manifested by both families converging to the $k_3 = 1$ asymptote. On the other hand, there exist families 5 and 6 which correspond to the families 5 and 6 of Figure 9. We see that they exist only for $k_3 \geqslant 1$ being a product of a saddle-node bifurcation occurring at $k_3 = 1$. Although these are k_2, k_3-parameter solution families for (95), they constitute an isolated solution of Eqs. (18).

♯ of Family	Branch description		
	φ_1	φ_2	φ_3
1	①	①	②
2	②	①	①
3	③	②	④
4	④	②	③
5	⑤	③	⑤
6	⑥	④	⑥

Table 6: The solution families depicted in Figure 10.

A special note must be made for the special case $k_2 = 0$. For this value of k_2 the only families that exist for $k_3 \neq 0$ are the families 5 and 6 of Figure 10 as it can be shown also in Figure 9. In this particular case it is also true that $\varphi_1 = \varphi_2 = \varphi_3$.

The fact that for this choice of k_2 and for $k_3 = 1$ we get the symmetric vortex solution $\Phi^{(\mathrm{sv})}{}_{101}$ both as a member of the

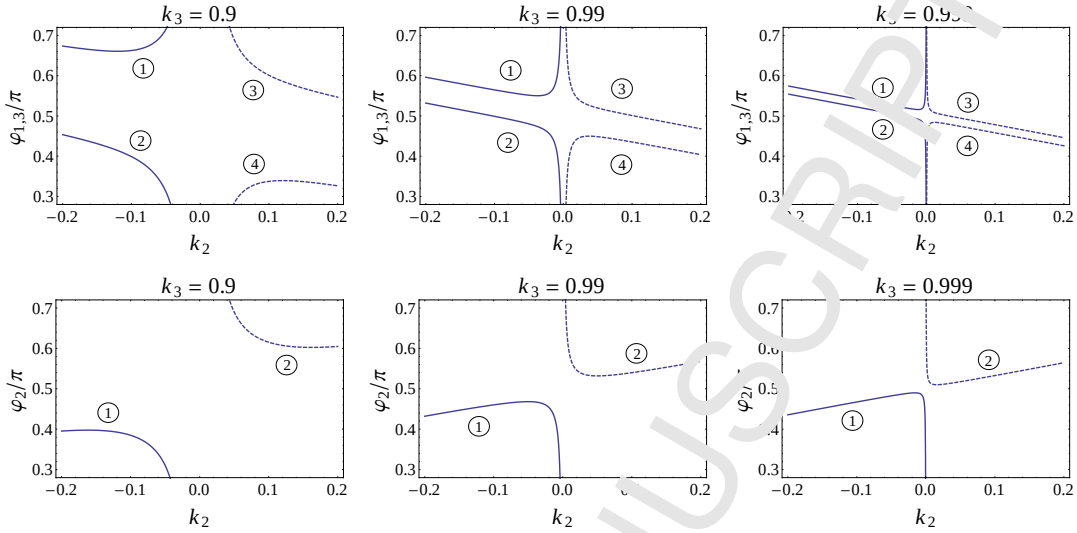

Figure 8: The bifurcation diagrams of the persistence condition (95), in the k-parameter region corresponding to the $\mathscr{H}_{101}$ model and in the $\boldsymbol{\varphi}$-region of $\Phi^{(\mathrm{sv})}$. The columns of the figure correspond to three distinct values of k_3, i.e. $k_3 = 0.9, 0.99, 0.999$, where the diagrams for an interval of k_2 in the specific region are shown. The upper row corresponds to the values of φ_1 and φ_3 of the solution-families while the bottom row depicts ϕ_2. Although the diagrams for φ_1 and φ_3 coincide geometrically, they do not have the same values in the corresponding families. The exact combination of branches for each family can be found in Table 4. We can observe how the various solution families converge to the $k_2 = 0$ asymptote, as $k_3 \to 1$.

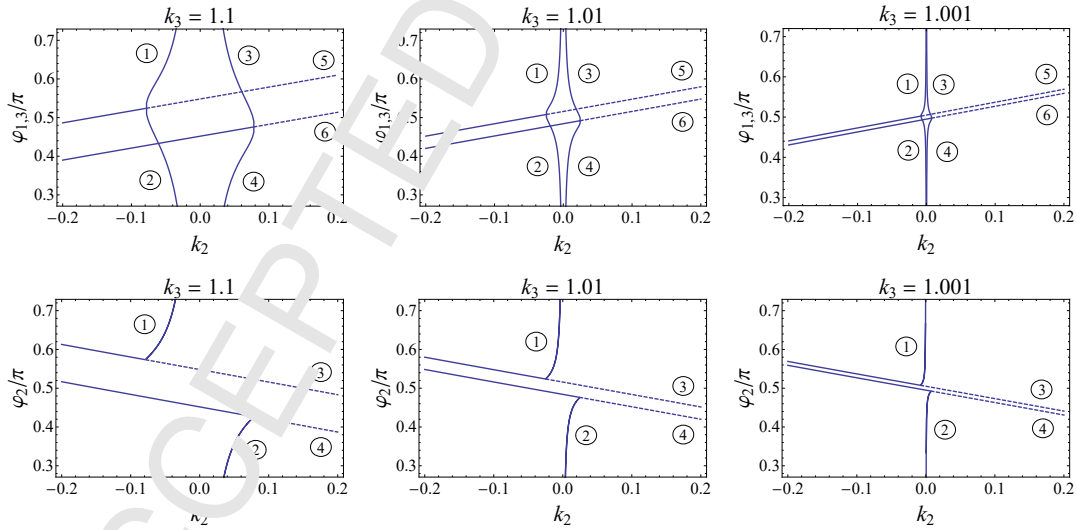

Figure 9: The bifurcation diagrams of the persistence condition (95), in the k-parameter region corresponding to the $\mathscr{H}_{101}$ model and in the $\boldsymbol{\varphi}$-region of $\Phi^{(\mathrm{sv})}$. The columns of the figure correspond to three distinct values of k_3, i.e. $k_3 = 1.1, 1.01, 1.001$, where the diagrams for an interval of k_2 in the specific region are shown. The upper row correspond to the values of φ_1 and φ_3 of the solution-families while the bottom row depicts ϕ_2. Although the diagrams for φ_1 and φ_3 coincide geometrically, they do not have the same values in the corresponding families. The exact branches which correspond to the different families are shown in Table 5. Note that, as $k_3 \to$, the families converge to the vortex families.

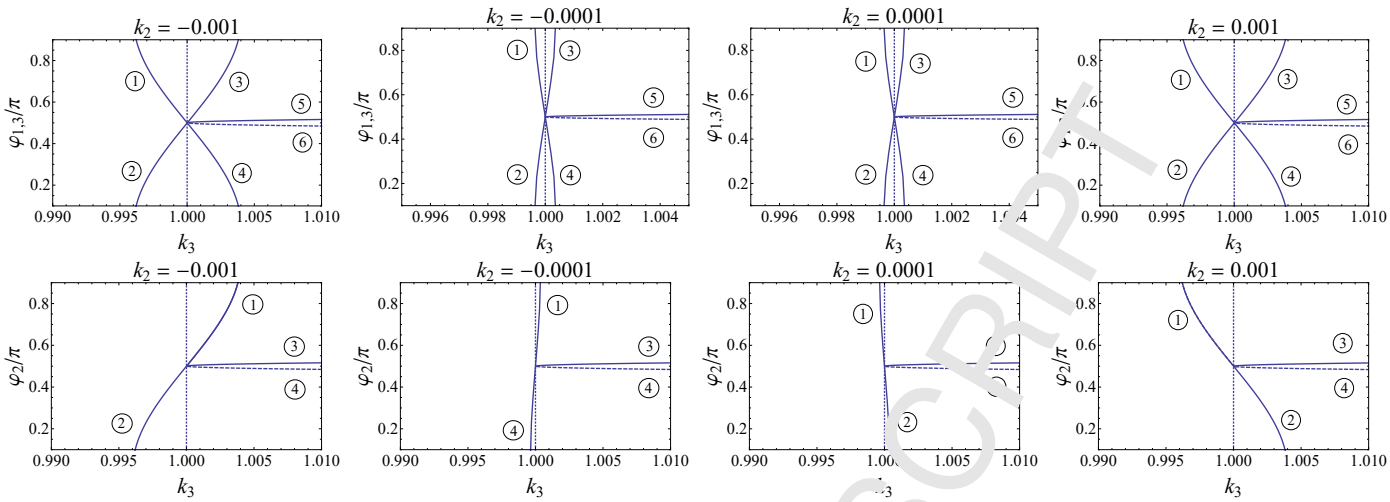

Figure 10: The bifurcation diagrams of the persistence condition (95), in the k-parameter region corresponding to the $\mathscr{H}_{101}$ model and in the $\boldsymbol{\varphi}$-region of $\Phi^{(\mathrm{sv})}$. The columns of the figure correspond to distinct values of k_2, while we have considered an interval of k_3 in the specific region. The upper row correspond to the values of φ_1 and φ_3 of the solution-families while φ_1 and φ_3 are coincide geometrically, they do not have the same values in the corresponding family. The exact branch combinations of φ_is are shown in Table 6. The family $F_2 : (\varphi, \pi - \varphi, \varphi)$ is degenerate and it is represented by a dotted line at $k_3 = 1$. Note how all the families, except of the "parabolic" one, converge to the $k_3 = 1$ asymptote, as $k_2 \to 0$.

vertical families and as a member of the "parabolic" family, numerically poses the question of the existence of the symmetric vortex solution in the real system. This question is also triggered by the fact that the two-dimensional analogue of our system in the dNLS limit it has been shown that vortices persist up to the (high) orders considered in [41].

We summarize the results of the previous numerical investigation, by saying that the persistence condition provide three one-parameter families of candidate MBs, instead of the two families for the $\mathscr{H}_{110}$ case. Each family carries two standard in-phase/out-of-phase solutions (whose existence is guaranteed via other approaches, [43]) and the three intersect in two highly symmetric objects, having $\boldsymbol{\varphi} = \Phi^{(\mathrm{sv})}_{01}$ and emulating two-dimensional vortices. The same kind of scenario and consequent degeneracy is shared by the corresponding beyond-nearest-neighbor discrete NLS approximation

$$H_{101} = \sum_j |\psi_j|^2 + \frac{3}{8}\sum_j |\psi_j|^4 + \frac{\epsilon}{2}\sum_j \left[|\psi_{j+1} - \psi_j|^2 + |\psi_{j+2} - \psi_j|^2\right], \tag{96}$$

examined systematically in [45]. It is thus natural to attempt transferring the nonexistence results there obtained previously by means of an accurate mathematical analysis. However, the techniques developed in Section 3 of the present paper are tailored for less degenerate models as it is also discussed in Section 4.

6. Conclusions - Future Directions

The present paper represents a natural follow up of [45], where we studied the related problem of the nonexistence of degenerate phase-shift discrete solitons in a beyond-nearest-neighbor dNLS lattice. We recall that in [45] the nonexistence of phase-shift discrete solitons, which was not easily achievable by means of averaging methods due to the degeneracy of the problem, was obtained in an efficient way by exploiting the rotational symmetry of the model and the density current conservation along the spatial profile of any candidate soliton. The absence of these ingredients in Klein-Gordon models represents an additional layer of difficulty to the degeneracy that one has to face in the continuation problem that we here address.

Keeping in mind the connections among these two classes of Hamiltonian models (KG and dNLS), a natural (although indirect) way to proceed is to transfer the results which are accessible in the dNLS context to similar results which are expected to be valid in the KG context, keeping track of the relevant correction terms. In this work we examined mainly KG systems with interactions beyond nearest neighbor interactions inspired, in part, by connections with higher dimensional lattices), with special emphasis on the zigzag model. In these models, by means of Lyapunov-Schmidt techniques, we showed that this approach actually works provided some smallness assumptions are made on the main physical parameters of the models: the energy E and the coupling strength ϵ.

However, the strategy presented here, is based on a first order normal form approximation of the KG model, and thus it has some limitations in cases where higher order degeneracies occur. In order to showcase this fact we shortly examine a model that exhibits next-to-next nearest neighbors interactions, namely the $\mathscr{H}_{101}$ model. Although the previously described methodology cannot be applied there, the numerical exploration performed in the Section 5.2 shows elements which strongly overlap with those that one can obtain in the corresponding dNLS normal form H_{101}, for which a rigorous answer has been given already in [45]. This naturally leads us to conjecture that a corresponding nonexistence statement of phase-shift four-site multibreathers holds true also for $\mathscr{H}_{101}$.

In order to prove such a conjecture, one could still follow this indirect approach, but attempt to increase the accuracy of the normal form approximation by adding further neighbor linear and nonlinear terms to the dNLS H_{101}, in the spirit of a

more general dNLS approximation (see [39, 40, 42]). Alternatively, one can use a more direct approach and perform a local normal form technique around the low-dimensional resonant torus, with the advantage of working directly in the original KG model without passing from the dNLS approximation (see [44] for the maximal tori case). With this scheme we expect to derive a normal form which naturally extends the effective Hamiltonian method introduced in [1]. In any case, and whatever the perturbation method one prefers to apply may be, it appears natural that the accuracy required in the approximation is directly related to the order of the degeneracy of the problem: hence, for highly degenerate problems the help of a computer assisted manipulation may be unavoidable and the choice of the method can become extremely relevant.

A related comment is that in the present work we have limited our considerations to one-dimensional settings with long-range interactions. Extending relevant ideas to genuinely higher-dimensional KG settings, where again the understanding built on the basis of the dNLS [23, 41] may be useful, is another natural avenue for future work. Indeed, in the two dimensional case significant degeneracies arise even in the homogeneous case, without the need to explore beyond nearest-neighbor interactions. Hence the problem of interest lies already at the level of the homogeneous 2d lattice. There, on the basis of the dNLS problem we expect degeneracies and hope to address the existence of solutions first in the easier dNLS case. Current numerical observations suggest the existence (even as robustly as to be experimentally observed) of discrete vortical structures. On the other hand, as already stressed in paragraph 4.3 about the $\mathcal{H}_{101}$ model, we suspect that the methods proposed herein may not be sufficient to tackle the transition between the dNLS and the KG case in all possible situations, hence further tools may need to be developed for the latter, depending on the geometry of the lattice and on the degree of degeneracy of the solutions of the bifurcation equations. An additional auxiliary set of models may be that of anisotropic coupling, starting with the so-called "railroad model" involving two "tracks" initially very weakly coupled and continuously varied until the equal coupling limit (which could be again explored numerically). These are some of the relevant directions examining further.

Acknowledgements

The authors, V.K., P.G.K., acknowledge that this work made possible by NPRP grant # [9-329-1-037] from Qatar National Research Fund (a member of Qatar Foundation). The findings achieved herein are solely the responsibility of the authors. Moreover, we warmly thank the reviewers for their comments on the first version of the manuscript, which have helped us to improve its accuracy and readability.

[1] T. Ahn, R.S. MacKay, and J.-A. Sepulchre. Dynamics of relative phases: Generalised multibreathers. *Nonlinear Dyn.*, 25(1-3):157–182, 2001. cited By 23.

[2] V.I. Arnol'd Proof of a theorem of A.N.Kolmogorov on the preservation of conditionally periodic motions under a small perturbation of the Hamiltonian. *Uspehi Mat. Nauk*, 18, no. 5 (113):13-40, 1963.

[3] S. Aubry. Breathers in nonlinear lattices: existence, linear stability and quantization. *Phys. D*, 103(1-4):201–250, 1997. Lattice dynamics (Paris, 1995).

[4] D. Bambusi, S. Paleari, and T. Penati. Existence and continuous approximation of small amplitude breathers in 1D and 2D Klein-Gordon lattices. *Appl. Anal.*, 89(9):1313–1334, 2010.

[5] M. Berti. *Nonlinear oscillations of Hamiltonian PDEs*. Progress in Nonlinear Differential Equations and their Applications, 74. Birkhäuser Boston, Inc., Boston, MA, 2007.

[6] P. Binder, D. Abraimov, A. V. Ustinov, S. Flach, and Y. Zolotaryuk. Observation of breathers in josephson ladders. *Phys. Rev. Lett.*, 84:745–748, Jan 2000.

[7] N. Boechler, G. Theocharis, C. Job, P. G. Kevrekidis, Mason A. Porter, and C. Daraio. Discrete breathers in one-dimensional diatomic granular crystals. *Phys. Rev. Lett.*, 104:244302, Jun 2010.

[8] D. K. Campbell, S. Flach, and Yu. S. Kivshar. Localizing energy through nonlinearity and discreteness. *Physics Today*, 57:43–49, 2004.

[9] C. Chong, F. Carretero-González, B. A. Malomed, and P. G. Kevrekidis. Variational approximations in discrete nonlinear Schrödinger equations with next-nearest-neighbor couplings. *Phys. D*, 240(14-15):1205–1212, 2011.

[10] C. Chong, F. Li, J. Yang, M. O. Williams, I. G. Kevrekidis, P. G. Kevrekidis, and C. Daraio. Damped-driven granular chains: An ideal playground for dark breathers and multibreathers. *Phys. Rev. E*, 89:032924, Mar 2014.

[11] T. Cretegny and S. Aubry. Spatially inhomogeneous time-periodic localized propagating waves in anharmonic systems. *Phys. Rev. B*, 57:R11929–R11932, May 1997.

[12] J. Cuevas, L. Q. English, P. G. Kevrekidis, and M. Anderson. Discrete breathers in a forced-damped array of coupled pendula: Modeling, computation, and experiment. *Phys. Rev. Lett.*, 102:224101, Jun 2009.

[13] J. Cuevas, V. Koukouloyannis, P. G. Kevrekidis, and J. F. R. Archilla. Multibreather and vortex breather stability in klein-gordon lattices: equivalence between two different approaches. *Int. J. Bifurc. Chaos*, 21(08):2161–2177, 2011.

[14] S.V. Dmitriev, E.A. Korznikova, Yu.A. Baimova and M.G. Velarde Discrete breathers in crystals. *Physics-Uspekhi*, 59(5):446, 2016.

[15] N.K. Efremidis and D.N. Christodoulides. Discrete solitons in nonlinear zigzag optical waveguide arrays with tailored diffraction properties. *Phys. Rev. E*, 65:056607, May 2002.

[16] L. Q. English, R. Basu Thakur, and Ryan Stearrett. Patterns of traveling intrinsic localized modes in a driven electrical lattice. *Phys. Rev. E*, 77:066601, Jun 2008.

[17] S. Flach, K. Kladko, and R. S. MacKay. Energy thresholds for discrete breathers in one-, two-, and three-dimensional lattices. *Phys. Rev. Lett.*, 78:1207–1210, Feb 1997.

[18] S. Flach and A.V. Gorbach. Discrete breathers advances in theory and applications. *Phys. Rep.*, 467(1):1 – 116, 2008.

[19] A. Giorgilli, U. Locatelli. Kolmogorov theorem and classical perturbation theory. *Zeitschrift für angewandte Mathematik und Physik ZAMP*, 48(2):220–261, Mar 1997.

[20] M. Golubitsky and D.G. Schaeffer. *Singularities and groups in bifurcation theory. Vol. I*, volume 51 of *Applied Mathematical Sciences*. Springer-Verlag, New York, 1985.

[21] T. Kapitula. Stability of waves in perturbed Hamiltonian systems. *Phys. D*, 156(1-2):186–200, 2001.

[22] T. Kapitula and P. Kevrekidis. Stability of waves in discrete systems. *Nonlinearity*, 14(3):533–566, 2001.

[23] P.G. Kevrekidis. *The discrete nonlinear Schrödinger equation*, volume 232 of *Springer Tracts in Modern Physics*. Springer-Verlag, Berlin, 2009. Mathematical analysis, numerical computations and physical perspectives.

[24] P.G. Kevrekidis. Non-nearest-neighbor interactions in nonlinear dynamical lattices. *Phys. Lett. A*, 373(40):3688–3693, 2009. cited By 5.

[25] P.G. Kevrekidis, D.J. Frantzeskakis, and R. Carretero-González. *Emergent Nonlinear Phenomena in Bose-Einstein Condensates*. Springer Series on Atomic, Optical and Plasma Physics. Springer-Verlag, Heidelberg, 2008.

[26] A.N. Kolmogorov Preservation of conditionally periodic move-

ments with small change in the Hamilton function. *Stochastic behavior in classical and quantum Hamiltonian systems (Volta Memorial Conf., Como, 1977)*: 51–56, Lecture Notes in Phys., 93, Springer, Berlin-New York, 1979.

[27] V Koukouloyannis, P G Kevrekidis, K J H Law, I Kourakis, and D J Frantzeskakis. Existence and stability of multisite breathers in honeycomb and hexagonal lattices. *J. Phys. A*, 43(23):235101, 2010.

[28] V. Koukouloyannis, P.G. Kevrekidis, K.J.H. Law, I. Kourakis, and D.J. Frantzeskakis. Existence and stability of multisite breathers in honeycomb and hexagonal lattices. *J. Phys. A*, 43(23):235101, 16, 2010.

[29] V. Koukouloyannis, P.G. Kevrekidis, J. Cuevas, and V. Rothos. Multibreathers in Klein-Gordon chains with interactions beyond nearest neighbors. *Phys. D*, 242(1):16 – 29, 2013.

[30] V. Koukouloyannis. Non-existence of phase-shift breathers in one-dimensional Klein-Gordon lattices with nearest-neighbor interactions. *Phys. Lett. A*, 377(34-36):2022–2026, 2013.

[31] V. Koukouloyannis and S. Ichtiaroglou. Existence of multi-breathers in chains of coupled one-dimensional Hamiltonian oscillators. *Phys. Rev. E (3)*, 66(6):066602, 8, 2002.

[32] V. Koukouloyannis and P.G. Kevrekidis. On the stability of multibreathers in Klein-Gordon chains. *Nonlinearity*, 22(9):2269–2285, 2009.

[33] V. Koukouloyannis and R.S. MacKay Existence and stability of 3-site breathers in a triangular lattice. *J. Phys. A*, 38(5):1021 – 1030, 2005.

[34] F. Lederer, G.I. Stegeman, D.N. Christodoulides, G. Assanto, M. Segev, and Y. Silberberg. Discrete solitons in optics. *Phys. Rep.*, 463(1):1 – 126, 2008.

[35] R S MacKay and S Aubry. Proof of existence of breathers for time-reversible or hamiltonian networks of weakly coupled oscillators. *Nonlinearity*, 7(6):1623, 1994.

[36] R.S. MacKay and J-A. Sepulchre. Effective Hamiltonian for travelling discrete breathers. *J. Phys. A*, 35(18):3985–4002, 2002.

[37] E. Meletlidou and G. Stagika. On the continuation of degenerate periodic orbits in Hamiltonian systems. *Regul. Chaotic Dyn.*, 11(1):131–138, 2006.

[38] J. Moser. Periodic orbits near an equilibrium and a theorem by Alan Weinstein. *Comm. Pure Appl. Math.*, 29(6):724–747, 1976.

[39] S. Paleari and T. Penati. An extensive resonant normal form for an arbitrary large Klein-Gordon model. *Ann. Mat. Pura Appl. (4)*, 195(1):133–165, 2016.

[40] S. Paleari and T. Penati. Long time stability of small-amplitude breathers in a mixed FPU-KG model. *Z. Angew. Math. Phys.*, 67(6):Art. 148, 21, 2016.

[41] D. E. Pelinovsky, P. G. Kevrekidis, and D. J. Frantzeskakis. Persistence and stability of discrete vortices in nonlinear Schrödinger lattices. *Phys. D*, 212(1-2):20–53, 2005.

[42] D. Pelinovsky, T. Penati, and S. Paleari. Approximation of small-amplitude weakly coupled oscillators by discrete nonlinear Schrödinger equations. *Rev. Math. Phys.*, 28(7):1650015, 25, 2016.

[43] D. Pelinovsky and A. Sakovich. Multi-site breathers in Klein-Gordon lattices: stability, resonance and bifurcations. *Nonlinearity*, 25(12):3423–3451, 2012.

[44] T. Penati, M. Sansottera, and V. Danesi. On the continuation of degenerate periodic orbits via normal form: full dimensional resonant tori. *Commun. Nonlinear Sci. Numer. Simul.*, 61:198–224, 2018.

[45] T. Penati, M. Sansottera, S. Paleari, V. Koukouloyannis, and P.G. Kevrekidis. On the nonexistence of degenerate phase-shift discrete solitons in the dNLS nonlocal lattice. *Phys. D*, page 10.1016/j.physd.2017.12.012, 2017.

[46] H. Poincaré. *Les méthodes nouvelles de la mécanique céleste. Tome I. Solutions périodiques. Non-existence des intégrales uniformes. Solutions asymptotiques.* Dover Publications, Inc., New York, N.Y., 1957.

[47] H. Poincaré. *Œuvres. Tome VII.* Les Grands Classiques Gauthier-Villars. [Gauthier-Villars Great Classics]. Éditions Jacques Gabay, Sceaux, 1996. Masses fluides en rotation. Principes de mécanique analytique. Problème des trois corps. [Rotating fluid masses. Principles of analytic mechanics. Three-body problem], With a preface by Jacques Lévy, Reprint of the 1952 edition.

[48] M. Sato, B. E. Hubbard, L. Q. English, A. J. Sievers, B. Ilic, D. A. Czaplewski, and H. G. Craighead. Study of intrinsic localized vibrational modes in micromechanical oscillator arrays. *Chaos*, 13(2):702–715, 2003.

[49] M. Sato, B. E. Hubbard, A. J. Sievers, B. Ilic, D. A. Czaplewski, and H. G. Craighead. Observation of locked intrinsic localized vibrational modes in a micromechanical oscillator array. *Phys. Rev. Lett.*, 90:044102, Jan 2003.

[50] U. T. Schwarz, L. Q. English, and A. J. Sievers. Experimental generation and observation of intrinsic localized spin wave modes in an antiferromagnet. *Phys. Rev. Lett.*, 83:223–226, Jul 1999.

[51] D.V. Treshchev. The mechanism of destruciton of resonant tori of Hamiltonian systems. *Math. USSR Sb.*, 68:181–203, 1991.

[52] E. Trias, J. J. Mazo, and T. P. Orlando. Discrete breathers in nonlinear lattices: Experimental detection in a josephson array. *Phys. Rev. Lett.*, 84:741–744, Jan 2000.

[53] G. Voyatzis, S. Ichtiaroglou. Degenerate bifurcations of resonant tori in Hamiltonian systems. *Internat. J. Bifur. Chaos Appl. Sci. Engrg.*, 9(5):849–863, 1999.

[54] A. Weinstein. Normal modes for nonlinear Hamiltonian systems. *Invent. Math.*, 20:47–57, 1973.

[55] L. Xu, Y. Li, Y. Yi. Poincaré-Treshchev Mechanism in Multi-scale, Nearly Integrable Hamiltonian Systems *J. Nonlin. Sc.*, 28(1):337–369, 2018.

PROPOSED HIGHLIGHTS:

- Klein-Gordon lattices with interactions beyond nearest-neighbor are examined.
- Existence and nonexistence conditions for degenerate phase-shift multibreathers are discussed.
- The correspondence between solutions in the KG and DNLS models is analyzed.
- Nonexistence of four-sites vortex-like structures in the zigzag Klein-Gordon lattice is established.